

Platinum(IV) Metallacrown Ethers: Synthesis, Structures, Host Properties and Anticancer Evaluation

Mairéad E. Kelly,[†] Andrea Dietrich,[‡] Santiago Gómez-Ruiz,[§] Bernd Kalinowski,[⊥] Goran N. Kaluderović,^{†,□} Thomas Müller,[‡] Reinhard Paschke,[⊥] Jürgen Schmidt,[△] Dirk Steinborn,[†] Christoph Wagner,[†] and Harry Schmidt^{*†}

Institut für Chemie, Martin-Luther-Universität Halle-Wittenberg, Kurt-Mothes-Strasse 2, 06120 Halle, Germany, Hämatologisch/Onkologisches Forschungslabor, KIM IV, Martin-Luther-Universität Halle-Wittenberg, Ernst-Grube-Strasse 40, 06120 Halle, Germany, Departamento de Química Inorgánica y Analítica, Universidad Rey Juan Carlos, Móstoles 28933, Madrid, Spain, Biozentrum, Martin-Luther-Universität Halle-Wittenberg, Weinbergweg 22, 06120 Halle, Germany, Department of Chemistry, Institute of Chemistry, Technology and Metallurgy, Studentski trg 14, 11000 Belgrade, Serbia, and Leibniz-Institut für Pflanzenbiochemie, Weinberg 3, 06120 Halle, Germany

Received April 10, 2008

Platinum(IV) metallacrown ethers [PtBr₂Me₂{im(CH₂CH₂O)_xCH₂CH₂im}] (im = imidazol-1-yl; x = 2–5, 7; **3–7**) and [PtBr₂Me₂{bim(CH₂CH₂O)_xCH₂CH₂bim}] (bim = benzimidazol-1-yl; x = 1, 2, 5, 7; **9–12**) were synthesized via the reaction of [(PtBr₂Me₂)_n] with the appropriate α,ω-bis(imidazol-1-yl) or α,ω-bis(benzimidazol-1-yl) polyether. Reactions with 1,2-bis(imidazol-1-yl)ethane, bis(2-(imidazol-1-yl)ethyl) ether, or 1,2-bis(benzimidazol-1-yl)ethane yielded the dinuclear complexes [(PtBr₂Me₂)₂{μ-im(CH₂CH₂O)_xCH₂CH₂im}]₂ (x = 0, 1; **1, 2**) and [(PtBr₂Me₂)₂{μ-bimCH₂CH₂bim}]₂ (**8**), respectively. In addition, the diiodo complex [PtI₂Me₂{im(CH₂CH₂O)₂CH₂CH₂im}] (**13**) was prepared from the reaction of [PtMe₂(cod)] with I₂ in the presence of im(CH₂CH₂O)₂CH₂CH₂im. Characterization by microanalysis and NMR spectroscopy, as well as X-ray crystal structure analysis of several of the metallacrown ethers (**3, 5, 9** and **10**) and dinuclear complexes (**2** and **8**), is described. The ability of the larger metallacrown ethers (**5–7, 11** and **12**) to act as hosts to either dibenzyl- or di-*n*-butylammonium ions is investigated in solution (NMR and ESI-MS). Finally, several of these metallacrown ethers were found to possess *in vitro* antitumor activity on three tumor cell lines (liposarcoma, A549 and 518A2). The activity of these complexes, all of which were found to induce apoptotic cell death, is discussed relative to their structure and the findings of platinum uptake studies.

1. Introduction

The area of metallomacrocycles has experienced significant attention over the last 20 years owing to the interesting magnetic, electronic and receptor properties these compounds demonstrate.¹ Metallacrowns are structures analogous to crown ethers but with $-[M-N-O]_n-$ (M is a transition metal) repeating units in a cyclic arrangement such that the nitrogen and transition metal atoms replace the methylene carbons of the crown ether.^{1d,f} On the other hand, metallacrown ethers are a class of metallomacrocycles that can be prepared through a ring-closing reaction between a ditopic ligand, usually with phosphine functionalities at the extremities of a polyether chain, and a

transition metal fragment. A number of such metallacrown ethers with ligating phosphine groups have been prepared incorporating Mo(0), Ru(II), Pd(II) and Pt(II) metal atoms.² An alternative ligand type with ligating nitrogen atoms from pyrazolyl moieties at the extremities has also been used to coordinate Ag(I) into the resulting metallacrown ether ring.³ More recently Ag(I), Au(I) and Hg(II) metallacrown ethers with ligating *N*-heterocyclic carbene moieties have been described.⁴ The ability of metallacrown ethers to behave as receptors for metal cations has been demonstrated and verified in the solid state.^{2a,d,5} While the interaction of ammonium ions with crown ethers is well studied⁶ and the interaction of these ions with metallacrowns

* To whom correspondence should be addressed. E-mail: h.schmidt@chemie.uni-halle.de.

[†] Institut für Chemie, Martin-Luther-Universität Halle-Wittenberg.

[‡] Hämatologisch/Onkologisches Forschungslabor, KIM IV, Martin-Luther-Universität Halle-Wittenberg.

[§] Universidad Rey Juan Carlos.

[⊥] Biozentrum, Martin-Luther-Universität Halle-Wittenberg.

[□] Institute of Chemistry, Technology and Metallurgy, Belgrade, Serbia.

[△] Leibniz-Institut für Pflanzenbiochemie.

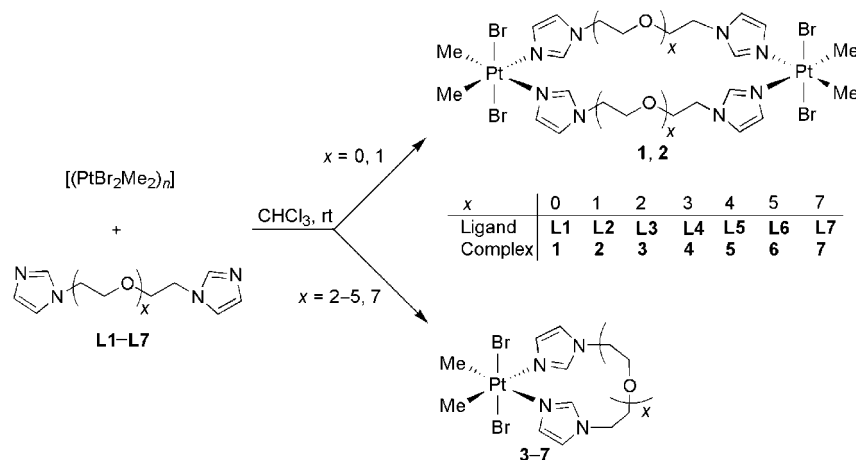
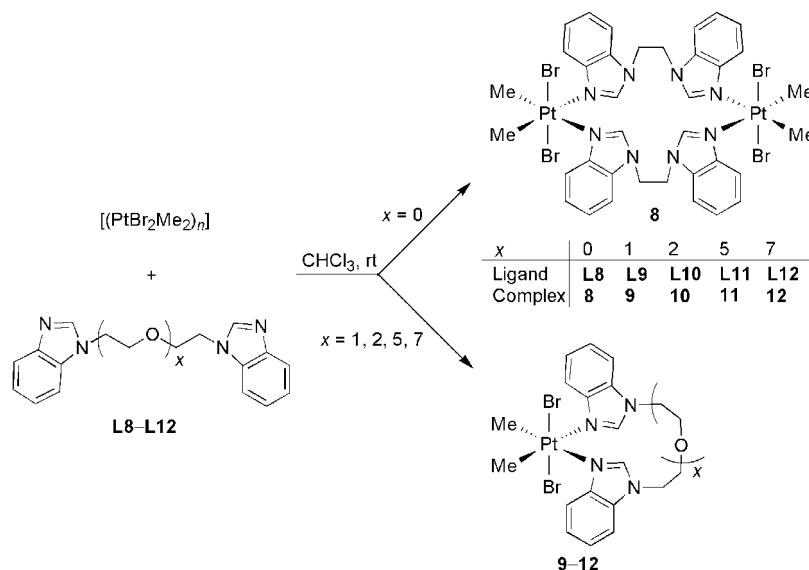
(1) (a) Leininger, S.; Olenyuk, B.; Stang, P. J. *Chem. Rev.* **2000**, *100*, 853. (b) Holliday, B. J.; Mirkin, C. A. *Angew. Chem., Int. Ed.* **2001**, *40*, 2022. (c) Swiegers, G. F.; Malefetse, T. J. *Chem. Rev.* **2000**, *100*, 3483. (d) Pecoraro, V. L.; Stemmler, A. J.; Gibney, B. R.; Bodwin, J. J.; Wang, H.; Kampf, J. W.; Barwinski, A. *Prog. Inorg. Chem.* **1997**, *45*, 83. (e) Slone, R. V.; Benkstein, K. D.; Bélanger, S.; Hupp, J. T.; Guzei, I. A.; Rheingold, A. L. *Coord. Chem. Rev.* **1998**, *171*, 221. (f) Mezei, G.; Zaleski, C. M.; Pecoraro, V. L. *Chem. Rev.* **2007**, *107*, 4933.

(2) (a) Butler, J. M.; Jablonsky, M. J.; Gray, G. M. *Organometallics* **2003**, *22*, 1081. (b) Gray, G. M.; Varshney, A.; Duffey, C. H. *Organometallics* **1995**, *14*, 238. (c) Smith, D. C., Jr.; Lake, C. H.; Gray, G. M. *Dalton Trans.* **2003**, 2950. (d) Varshney, A.; Webster, M. L.; Gray, G. M. *Inorg. Chem.* **1992**, *31*, 2580.

(3) Grosshans, P.; Jouaiti, A.; Hosseini, M. W.; De Cian, A.; Kyrtsakos-Gruber, N. *Tetrahedron Lett.* **2003**, *44*, 1457.

(4) (a) Wang, J.-W.; Li, Q.-S.; Xu, F.-B.; Song, H.-B.; Zhang, Z.-Z. *Eur. J. Org. Chem.* **2006**, 1310. (b) Liu, Q.-X.; Zhao, X.-J.; Wu, X.-M.; Guo, J.-H.; Wang, X.-G. *J. Organomet. Chem.* **2007**, *692*, 5671.

(5) (a) Gray, G. M.; Duffey, C. H. *Organometallics* **1995**, *14*, 245. (b) Gray, G. M.; Fish, F. P.; Duffey, C. H. *Inorg. Chim. Acta* **1996**, *246*, 229. (c) Varshney, A.; Gray, G. M. *Inorg. Chem.* **1991**, *30*, 1748. (d) Powell, J.; Lough, A.; Wang, F. *Organometallics* **1992**, *11*, 2289. (e) Bélanger, S.; Gilbertson, M.; Yoon, D. I.; Stern, C. L.; Dang, X.; Hupp, J. T. *J. Chem. Soc., Dalton Trans.* **1999**, 3407.

Scheme 1. Preparation of 1–7 by Reaction of α,ω -Bis(imidazol-1-yl) Polyether Ligands L1–L7 with $[(\text{PtBr}_2\text{Me}_2)_n]$ Scheme 2. Preparation of 8–12 by Reaction of α,ω -Bis(benzimidazol-1-yl) Polyether Ligands L8–L12 with $[(\text{PtBr}_2\text{Me}_2)_n]$ 

is often employed in their synthesis,⁷ their behavior with metallacrown ethers has received little attention.^{5c}

In addition to receptor properties, the inclusion of polyether chains in transition metal complexes may be expected to lend these complexes better to hydrophilic environments, a feature

attractive in drug design. Incorporation of crown ether type ligands in anticancer platinum drugs has been demonstrated by a number of authors.⁸ Organometallic complexes, particularly of Fe and Ru, that show anticancer properties have attracted considerable attention in recent years.⁹ However reports on anticancer properties of organometallic platinum complexes are rare relative to those of cisplatin-like derivatives.¹⁰ Herein we report the preparation of a number of platinum(IV) metallacrown ethers having ligands with imidazol-1-yl (im) or benzimidazol-1-yl (bim) at the ligating terminals of a polyether chain. The capability of these metallacrown ethers to complex dialkylammonium ions was investigated in solution. In addition, *in vitro* anticancer activity of selected complexes from these platinum(IV) metallacrown ethers is reported for three tumor cell lines. The induced mode of cell death was also investigated and the anticancer activity of the compounds is discussed relative to their structure and the results of a drug uptake study.

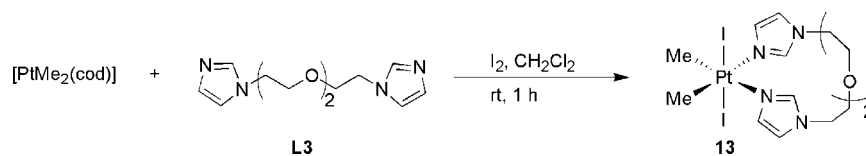
(6) See for example: (a) Pedersen, C. J. *J. Am. Chem. Soc.* **1967**, 7017. (b) Pedersen, C. J. *J. Am. Chem. Soc.* **1970**, 386. (c) Williams, A. R.; Northrop, B. H.; Houk, K. N.; Stoddart, J. F.; Williams, D. J. *Chem. Eur. J.* **2004**, 10, 5406. (d) Gokel, G. W.; Abel, E. In *Molecular Recognition: Receptors for Cationic Guests*; Gokel, G. W., Ed.; In Comprehensive Supramolecular Chemistry Vol. 1; Elsevier Science Ltd., BPC Wheatons Ltd.: Exeter, UK, 1996. (e) Gokel, G. *Crown Ethers and Cryptands*; Waldmann, O.; Timco, G. A.; Winpenny, R. E. P. *Chem. Commun.* **2005**, 1125. (f) Cador, O.; Gatteschi, D.; Sessoli, R.; Larsen, F. K.; Overgaard, J.; Barra, A.-L.; Teat, S. J.; Timco, G. A.; Winpenny, R. E. P. *Angew. Chem., Int. Ed.* **2004**, 43, 5196. (g) Larsen, F. K.; Overgaard, J.; Parsons, S.; Rentschler, E.; Smith, A. A.; Timco, G. A.; Winpenny, R. E. P. *Angew. Chem., Int. Ed.* **2003**, 42, 5978. (h) Larsen, F. K.; McInnes, E. J. L.; El Mkami, H.; Overgaard, J.; Piligkos, S.; Rajaraman, G.; Rentschler, E.; Smith, A. A.; Smith, G. M.; Boote, V.; Jennings, M.; Timco, G. A.; Winpenny, R. E. P. *Angew. Chem., Int. Ed.* **2003**, 42, 101. (i) Zhao, Y.; Zhu, G.; Liu, W.; Zou, Y.; Pang, W. *Chem. Commun.* **1999**, 2219.

(7) (a) Jones, L. F.; Barrett, S. A.; Kilner, C. A.; Halcrow, M. A. *Chem. Eur. J.* **2008**, 14, 223. (b) Timco, G. A.; Batsanov, A. S.; Larsen, F. K.; Muryn, C. A.; Overgaard, J.; Teat, S. J.; Winpenny, R. E. P. *Chem. Commun.* **2005**, 3649. (c) Laye, R. H.; Larsen, F. K.; Overgaard, J.; Muryn, C. A.; McInnes, E. J. L.; Rentschler, E.; Sanchez, V.; Teat, S. J.; Güdel, H.; Waldmann, O.; Timco, G. A.; Winpenny, R. E. P. *Chem. Commun.* **2005**, 1125. (d) Cador, O.; Gatteschi, D.; Sessoli, R.; Larsen, F. K.; Overgaard, J.; Barra, A.-L.; Teat, S. J.; Timco, G. A.; Winpenny, R. E. P. *Angew. Chem., Int. Ed.* **2004**, 43, 5196. (e) Larsen, F. K.; Overgaard, J.; Parsons, S.; Rentschler, E.; Smith, A. A.; Timco, G. A.; Winpenny, R. E. P. *Angew. Chem., Int. Ed.* **2003**, 42, 5978. (f) Larsen, F. K.; McInnes, E. J. L.; El Mkami, H.; Overgaard, J.; Piligkos, S.; Rajaraman, G.; Rentschler, E.; Smith, A. A.; Smith, G. M.; Boote, V.; Jennings, M.; Timco, G. A.; Winpenny, R. E. P. *Angew. Chem., Int. Ed.* **2003**, 42, 101. (g) Zhao, Y.; Zhu, G.; Liu, W.; Zou, Y.; Pang, W. *Chem. Commun.* **1999**, 2219.

(8) (a) Yoo, J.; Sohn, Y. S.; Do, Y. *J. Inorg. Biochem.* **1999**, 73, 187. (b) Gund, A.; Keppler, B. K. *Angew. Chem., Int. Ed. Engl.* **1994**, 33, 186.

(9) *Bioorganometallics: Biomolecules, Labeling, Medicine*; Jaouen, G., Ed.; Wiley-VCH Verlag GmbH & Co.: Weinheim, 2006.

(10) (a) Hambley, T. W.; Battle, T. W.; Deacon, A. R.; Lawrenz, G. B.; Fallon, E. T.; Gatehouse, G. D.; Webster, B. M.; Rainone, L. K. S. *J. Inorg. Biochem.* **1999**, 77, 3. (b) Lindner, R.; Kaluđerović, G. N.; Paschke, R.; Wagner, Ch.; Steinborn, D. *Polyhedron* **2008**, 27, 914. (c) Ma, D.-L.; Shum, T. Y.-T.; Zhang, F.; Che, C.-M.; Yang, M. *Chem. Commun.* **2005**, 4675.

Scheme 3. Preparation of **13** from [PtMe₂(cod)] and L3 in the Presence of I₂Table 1. Selected ¹H, ¹³C and ¹⁹⁵Pt NMR Data (δ in ppm, J in Hz) of **1–7** and **9–13**

complex	solvent	PtCH ₃	
		δ _H (² J _{Pt,H})	δ _C (¹ J _{Pt,C})
1	(CD ₃) ₂ CO	1.76 (71.0)	-10.8 ^a
2	(CD ₃) ₂ CO	1.79 (70.8)	-12.0 ^{ab}
3	CDCl ₃	1.91 (70.6)	-10.5 (506.0)
4	CDCl ₃	1.88 (70.6)	-10.6 (504.5)
5	CDCl ₃	1.89 (70.6)	-10.5 (506.3)
6	CDCl ₃	1.91 (70.8)	-10.6 (504.3)
7	CDCl ₃	1.88 (70.6)	-10.7 (504.1)
9	CD ₂ Cl ₂	2.40 (73.5)	-9.9 ^a
10	CD ₂ Cl ₂	2.16 (72.2)	-8.6 (516.4)
11	CDCl ₃	2.25 (71.8)	-8.3 (513.9)
12	CD ₂ Cl ₂	2.17 (71.6)	-8.1 (515.0)
13	CDCl ₃	2.32 (72.6)	-19.3 ^a

^a Coupling not observed. ^b Measured in CD₃CN. ^c Measured in (CD₃)₂CO.

2. Results and Discussion

2.1. Synthesis and Spectroscopic Characterization. Similar to other reactions with the precursor complex [(PtBr₂Me₂)_n],¹¹ α,ω-bis(imidazol-1-yl) polyether-type ligands (im(CH₂CH₂O)_x-CH₂CH₂im; x = 0–5 and 7; **L1–L7**) were combined with a suspension of [(PtBr₂Me₂)_n] in chloroform to yield the corresponding platinum(IV) complexes (**1–7**), as depicted in Scheme 1.

α,ω-Bis(benzimidazol-1-yl) polyether-type ligands (bim(CH₂-CH₂O)_x-CH₂CH₂bim; x = 0, 1, 2, 5, 7; **L8–L12**) were used to prepare the respective dibromodimethylplatinum(IV) complexes (**8–12**), as illustrated by Scheme 2. The diiodo complex [PtI₂Me₂(**L3**)] (**13**) was prepared by slight modification of a procedure (Scheme 3) described in the literature.¹²

Solid state structural analysis (see later) confirms the formation of the dinuclear products [(PtBr₂Me₂)₂(μ-**L2**)₂] (**2**) and [(PtBr₂Me₂)₂(μ-**L8**)₂] (**8**). Complex **1**, [(PtBr₂Me₂)₂(μ-**L1**)₂], is assigned as dinuclear by analogy with **8** due to the structural similarities of **L1** and **L8**. All other complexes of the series, including [PtBr₂Me₂(**L9**)] (**9**) yielded from the benzimidazolyl analogue of **L2**, are mononuclear (**3–7** and **9–13**). Complexes **1–13** are air stable and were obtained in high yields (72–100%).

Complexes **1–7** and **9–13** were characterized in solution by ¹H, ¹³C and ¹⁹⁵Pt NMR spectroscopy, and selected data are collected in Table 1. As mentioned, **8** proved too insoluble to allow characterization by NMR spectroscopy, but its X-ray crystal structure is discussed below. The reactivity of [(PtBr₂Me₂)_n] with nitrogen donors has been thoroughly investigated^{11a,13} and has been shown to afford complexes with *trans* coordination of the nitrogen donor ligands to the methyl ligands and a mutual *trans* configuration of the bromo ligands. Our NMR spectroscopic investigations were consistent with this coordination geometry. The ¹H NMR spectra of **1–7** and **9–13**

show a single resonance for Pt–CH₃ (δ_H 1.76–2.40 ppm) with a ²J_{Pt,H} coupling constant of 70.6–73.5 Hz. The corresponding resonance in the ¹³C NMR spectra (δ_C ca. -19 to -8 ppm) with a ¹J_{Pt,C} coupling constant of ca. 504–516 Hz confirms the aforementioned configuration for **1–7** and **9–12** as well as the analogous configuration of **13** (configuration index: OC–6–13).

The similar range of δ_{Pt} for **1–7** (ca. -2326 to -2362 ppm) and **9–12** (ca. -2306 to -2338 ppm) demonstrates the similarity of the electronic environment around the platinum atom in the imidazol-1-yl and benzimidazol-1-yl complexes. The high-field shift of the singlet resonance in the ¹⁹⁵Pt NMR spectrum of diiodo-substituted **13** (3/**13**: δ_{Pt} -2362/-2738 ppm) is in accordance with a trend observed for platinum complexes of many types where bromo ligands are substituted by iodo ligands.¹⁴ In addition the values of δ_{Pt} for **1–7** and **9–13** compare well with the shifts observed for other dihalodimethylplatinum(IV) complexes.^{11a,15} In more concentrated solutions of **7** and **12** a second species was observed by NMR spectroscopy (at 0.05 M ca. 10%). In both cases the second species was found to diminish and disappear on dilution. This concentration-dependent equilibrium probably involves the formation of cyclic dimers or oligomers, as has been found for other metallacrown ethers.¹⁶

2.2. Crystal Structure Analysis. From the series of complexes **1–13** single crystals of **2**·2THF, **3**·CHCl₃, **5**, **8**·2CH₂Cl₂, **9**·CHCl₃ and **10**·CH₂Cl₂ suitable for X-ray crystallographic measurement were obtained (Figures 1–6). Both **2**·2THF and **8**·2CH₂Cl₂ show a bridging mode of the respective ligands **L2** and **L8**, yielding dinuclear complexes, while the remaining structures verify a bidentate chelating mode of the respective polyether ligands, affording mononuclear complexes.

All structures show a roughly octahedral arrangement of ligator atoms [Br₂C₂N₂] around the central platinum atom. In accordance with the spectroscopic characterization in solution, the nitrogen donor ligands are coordinated *trans* to the methyl ligands and the bromo ligands are mutually *trans* configured.

The interplanar angles between the least-squares planes of the [PtC₂N₂] atoms and *N*-heterocyclic rings range between 40.8(1)° and 59.7(2)° in all structures. The bond lengths and angles of **2**·2THF, **3**·CHCl₃ and **5** (see Supporting Information, Tables S1 and S2) show no unusual deviations from the norm. This is also found to be true for most of the bond lengths of **8**·2CH₂Cl₂, **9**·CHCl₃ and **10**·CH₂Cl₂. The exception is the Pt–N3 bond (2.215(2) Å) of **10**·CH₂Cl₂, which is slightly longer than typical Pt(IV)–N bond lengths of this type (median 2.163 Å; lower/upper quartile 2.142/2.198 Å; n = 351; n = number of observations).¹⁷

(14) Pergosin, P. S. In *Transition Metal Magnetic Resonance*; Pergosin, P. S., Ed.; Studies in Inorganic Chemistry 13; Elsevier: Amsterdam, The Netherlands, 1991.

(15) Appleton, T. G.; D'Alton, C. J.; Hall, J. R.; Mathieson, M. T.; Williams, M. A. *Can. J. Chem.* **1996**, *74*, 2008.

(16) (a) Smith, D. C., Jr.; Gray, G. M. *Inorg. Chem.* **1998**, *37*, 1791. (b) Smith, D. C., Jr.; Gray, G. M. *J. Chem. Soc., Dalton Trans.* **2000**, 677.

(17) Cambridge Structural Database (CSD); University Chemical Laboratory, Cambridge.

(11) (a) Kelly, M. E.; Gómez-Ruiz, S.; Kluge, R.; Merzweiler, K.; Steinborn, D.; Wagner, Ch.; Schmidt, H. *Inorg. Chim. Acta*, published online. (b) Beagley, P.; Starr, E. J.; Basca, J.; Moss, J. R.; Hutton, A. T. *J. Organomet. Chem.* **2002**, *645*, 206.

(12) Clark, H. C.; Ferguson, G.; Jain, V. K.; Parvez, M. *Organometallics* **1983**, *2*, 806.

(13) Hall, J. R.; Swile, G. A. *J. Organomet. Chem.* **1973**, *56*, 419.

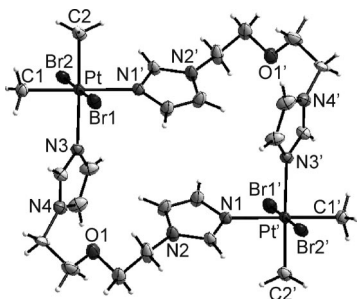


Figure 1. Molecular structure of dinuclear **2**·2THF, THF omitted. Displacement ellipsoids at 30% probability.

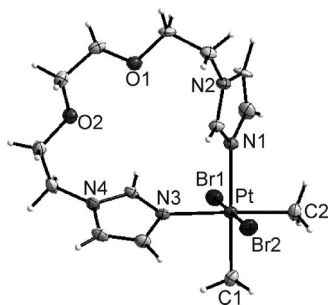


Figure 2. Molecular structure of **3**·CHCl₃, CHCl₃ omitted. Displacement ellipsoids at 30% probability.

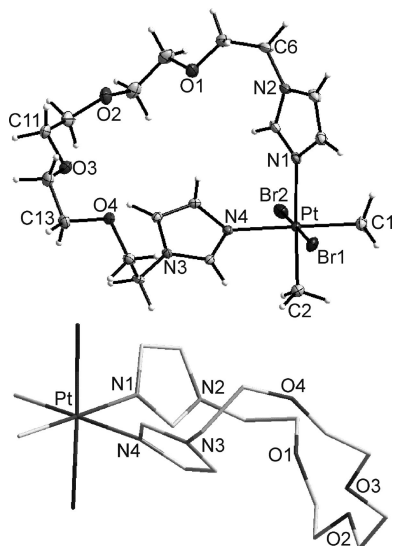


Figure 3. Molecular structure of **5**. Displacement ellipsoids at 30% probability and stick model showing orientation of the macro-ring.

As seen in Table 2, both **9**·CHCl₃ and **10**·CH₂Cl₂ show significant distortions from the ideal octahedral geometry. Indeed the N–Pt–N bond angles (ca. 85°) in both structures approach values typical for N–Pt–N bite angles in five-membered chelate rings (median 83.1°; lower/upper quartile 82.0/84.1°; *n* = 192). The Br–Pt–Br angles of **8**·2CH₂Cl₂ (176.2(1)° and 176.7(2)°) and that of **10**·CH₂Cl₂ (174.6(1)°) differ significantly from the typical range of values found for other hexacoordinated platinum(IV) complexes with nonbridging bromo ligands (median 179.7°; lower/upper quartile 177.7/180°; *n* = 37). Relative to the imidazol-1-yl structures, these deviations from the ideal angles are attributed to the increased bulk of the ligating benzimidazol-1-yl moiety.

Yellow needles of **5** (Figure 3) crystallized from a solution of **5** in the presence of KBF₄ and its structure is of particular

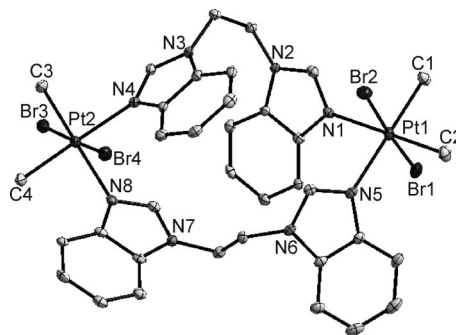


Figure 4. Molecular structure of dinuclear **8**·2CH₂Cl₂, hydrogen atoms and CH₂Cl₂ omitted. Displacement ellipsoids at 30% probability.

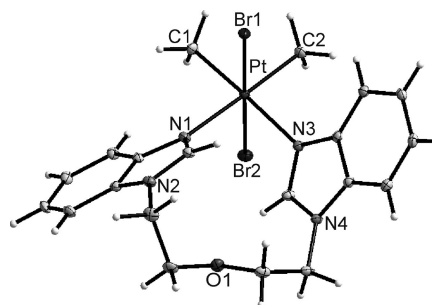


Figure 5. Molecular structure of **9**·CHCl₃, CHCl₃ omitted. Displacement ellipsoids at 30% probability.

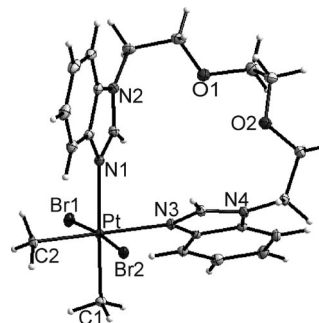


Figure 6. Molecular structure of **10**·CH₂Cl₂, CH₂Cl₂ omitted. Displacement ellipsoids at 30% probability.

Table 2. Selected Bond Angles [deg] of **8**·2CH₂Cl₂, **9**·CHCl₃ and **10**·CH₂Cl₂

	8 ·2CH ₂ Cl ₂	9 ·CHCl ₃	10 ·CH ₂ Cl ₂
C–Pt–C	87.6(2)	87.0(1)	88.4(1)
C–Pt–N	88.7(2)	179.2(2)	178.5(1)
N–Pt–N	179.3(2)	178.0(1)	177.4(1)
Br–Pt–Br	179.5(2)	179.7(1)	174.6(1)
	178.9(2)	85.6(1)	85.7(1)
	87.3(1)		
	87.2(1)		
	176.2(1)		
	176.7(1)		

interest since the binding properties of this complex were also investigated. The maximum dimensions of the cavity are given by the C6···C13 distance of 8.854(6) Å and the Pt···C11 distance of 8.378(4) Å. The O1···O4 distance of 6.143(1) Å is slightly larger than the same distance found for other metallacrown ethers with four ethyleneoxy groups, some of which have been shown to complex hard metal cations.^{2d,5b} Three of the four oxygen atoms are pointed inward on the metallacrown ether ring cavity, while O2 adopts a neutral

position directed neither inward nor outward relative to the macro-ring. Thus, both the size of the ring cavity in the structure of **5** and the orientation of the oxygen atoms indicate its potential to bind cations in the metallacrown ether ring cavity.

Finally, three of the four benzimidazolyl rings in each molecule of **8** (those coordinated via N1, N4 and N8) interact with their counterparts on three neighboring molecules via head-to-tail aromatic $\pi-\pi$ stacking.¹⁸ The characteristic parameters are very similar for all three interacting ring pairs. Taking the parameters between the imidazolyl-benzene portions of each interacting pair, the interplanar distances are between 3.35 and 3.48 Å, the centroid...centroid distances are between 3.63(1) and 3.77(1) Å and the displacement angles¹⁹ range from 20.6° to 23.4°. Similarly, one benzimidazolyl ring of **10** (coordinated through N1) and that of its counterpart on a neighboring molecule are also interacting via head-to-tail aromatic $\pi-\pi$ stacking. The interplanar distance is 3.42(1) Å, the centroid...centroid distance between pairs of parallel imidazolyl-benzene portions is 3.70(1) Å and the displacement angle is 23.2°.

2.3. Binding Studies. Dialkylammonium ions, depending on their constitution and that of the crown ether, can thread the cavity of a crown ether in a [2]pseudorotaxane-type interaction.^{6c,20} The ability of the metallacrown ethers **5–7**, **11** and **12** to behave as host molecules to dialkylammonium guests in solution (methylene chloride or chloroform) was studied with dibenzylammonium hexafluorophosphate, [Bn₂NH₂][PF₆], and di-*n*-butylammonium hexafluorophosphate, [Bu₂NH₂][PF₆].

A primary indicator of interaction is given by the considerably enhanced solubility of the dialkylammonium salts in methylene chloride in the presence of **5–7**, **11**, or **12**. One equivalent of either dialkylammonium salt is completely solubilized with **6**, **7** and **12**. This was also found to be the case for mixtures of **5** or **11** with [Bu₂NH₂][PF₆], but with either of these metallacrown ethers only approximately half an equivalent of [Bn₂NH₂][PF₆] goes into solution. With the exception of **12** + [Bn₂NH₂][PF₆], only one set of resonances is observed in the ¹H and ¹³C NMR spectra for the host-guest mixtures, rather than two sets assignable to complexed and free species in a slow exchange process. From the ¹H NMR spectrum of **12** + [Bn₂NH₂][PF₆] an estimate of the association constant ($K_a = 5 \text{ M}^{-1}$ in CD₂Cl₂ at 27 °C) by single-point determination²¹ demonstrates a weak binding interaction relative to crown ethers.^{20a}

Other than the observed enhanced solubility and changes in respective NMR spectra, evidence of complexation was also obtained using high-resolution ESI mass spectrometry. Relatively intense peaks corroborating a 1:1 binding ratio are found in the ESI-MS spectra of all respective mixtures (Supporting Information, Figure S1 and Table S4). Nuclear Overhauser

Table 3. Results of the Cytotoxicity Assay on the Three Tumor Cell Lines Liposarcoma, A549 (Lung Carcinoma) and 518A2 (Melanoma) Represented by the IC₅₀ [μM] Values^a

compound	IC ₅₀ [μM]		
	liposarcoma	A549	518A2
1	38.8 ± 18.4	9.7 ± 1.8	20.9 ± 5.2
2	7.8 ± 0.3	5.3 ± 0.3	6.7 ± 0.4
3	8.6 ± 0.0	7.2 ± 0.1	8.9 ± 0.0
6	4.0 ± 0.3	7.4 ± 0.2	7.1 ± 0.2
10	9.5 ± 7.0	12.8 ± 1.4	8.0 ± 3.6
13	13.7 ± 5.4	4.7 ± 3.1	9.5 ± 6.9
L1 ($x = 0$)	42.3 ± 21.5	37.6 ± 3.2	54.3 ± 24.2
L6 ($x = 5$)	> 150	> 150	> 150
[PtBr ₂ Me ₂ (DMF) ₂]	85.3 ± 35.2	94.9 ± 29.8	94.4 ± 37.6
cisplatin	0.130	0.163	0.179

^a Evaluation of cisplatin is under similar conditions. x = number of ethyleneoxy groups.

enhancement (NOE) experiments also confirm interaction between combinations of [Bu₂NH₂][PF₆] and all respective metallacrown ethers except **11**. NOE experiments also confirm an interaction between [Bn₂NH₂][PF₆] and the larger metallacrown ethers **12** and **7**, respectively (Supporting Information Table S3).

2.4. Anticancer Properties. The *in vitro* anticancer activity of selected compounds of the series **1–13** was investigated. Namely, complexes **1–3**, **6** and benzimidazol-1-yl and diiodo analogues of **3**, complexes **10** and **13**, were tested on the three tumor cell lines liposarcoma, A549 (nonsmall-cell lung carcinoma) and 518A2 (melanoma). The IC₅₀ data of these compounds, along with those of cisplatin, two of the ligands (**L1** and **L6**) and the solvated species [PtBr₂Me₂(DMF)₂], formed by [(PtBr₂Me₂)_{*n*}] in DMF,^{11a,13} are collected in Table 3. Although the activity of **1–3**, **6**, **10** and **13** is less than that of cisplatin on each cell line, it is clear that the complexes possess significant activity.

Comparing the activities of the free ligands with their corresponding complexes it was found that the activity of **L6** ($x = 5$ ethyleneoxy groups) exceeds the measurement range, while **6**, [PtBr₂Me₂(**L6**)], shows substantial activity on all three cell lines. The ethylene-linked **L1** ($x = 0$) shows moderate activity, and the corresponding complex **1**, [(PtBr₂Me₂)₂(μ -**L1**)₂], exhibits greater activity on the lung carcinoma A549 cell line only. The IC₅₀ values determined for **1** on both of the other cell lines fall within the same experimental range as **L1**. It is interesting to note that **L1** has been shown to influence the activity of carbonic anhydrases,²² enzymes that are prevalent in solid tumors.²³

Complexes bearing ethyleneoxy groups on the ligand backbone (**2**, **3**, **6**, **10** and **13**) show higher activity than [PtBr₂Me₂(DMF)₂] on all cell lines and higher activity than **1** on the 518A2 and liposarcoma cell lines. [PtBr₂Me₂(DMF)₂] indicates the activity of the PtBr₂Me₂ moiety in the absence of the polyether-type ligands. The level of activity of **2**, **3**, **6**, **10** and **13** is comparable on all cell lines. No major change in activity is observed between **2** [(PtBr₂Me₂)₂(μ -**L2**)₂] and **3** [PtBr₂Me₂(**L3**)]. Increasing the ligand backbone from two to

(18) (a) Janiak, C. J. *Chem. Soc., Dalton Trans.* **2000**, 3885. (b) Hunter, C. A.; Lawson, K. R.; Perkins, J.; Urch, C. J. *J. Chem. Soc., Perkin Trans.* **2001**, 651.

(19) Angle given by the vector between the centroids and the normal to the planes of the rings.

(20) See for example: (a) Ashton, P. R.; Campbell, P. J.; Chrystal, E. J. T.; Glink, P. T.; Menzer, S.; Philp, D.; Spencer, N.; Stoddart, J. F.; Tasker, P. A.; Williams, D. J. *Angew. Chem., Int. Ed. Engl.* **1995**, *34*, 1865. (b) Ashton, P. R.; Chrystal, E. J. T.; Glink, P. T.; Menzer, S.; Schiavo, C.; Stoddart, J. F.; Tasker, P. A.; Williams, D. J. *Angew. Chem., Int. Ed. Engl.* **1995**, *34*, 1869. (c) Bryant, W. S.; Guzei, I. A.; Rheingold, A. L.; Merola, J. S.; Gibson, H. W. *J. Org. Chem.* **1998**, *63*, 7634. (d) Chiu, S.-H.; Rowan, S. J.; Cantrill, S. J.; Stoddart, J. F.; White, A. J. P.; Williams, D. J. *Chem. Eur. J.* **2002**, *8*, 5170.

(21) Tsukube, H.; Furuta, H.; Odani, A.; Takeda, Y.; Kudo, Y.; Inoue, Y.; Liu, Y.; Sakamoto, H.; Kimura, K. In *Physical Methods in Supramolecular Chemistry*; Davies, J. E. D., Ripmeester, J. A., Eds.; Comprehensive Supramolecular Chemistry Vol. 8; Elsevier Science Ltd., BPC Wheatons Ltd.: Exeter, UK, 1996.

(22) (a) Supuran, C. T.; Balaban, A. T.; Cabildo, P.; Claramunt, R. M.; Lavandera, J. L.; Elguero, J. *Biol. Pharm. Bull.* **1993**, *16* (12), 1236. (b) Supuran, C. T.; Claramunt, R. M.; Lavandera, J. L.; Elguero, J. *Biol. Pharm. Bull.* **1996**, *19* (11), 1417.

(23) (a) Swinson, D. E. B.; Jones, J. L.; Richardson, D.; Wykoff, C.; Turley, H.; Pastorek, J.; Taub, N.; Harris, A. L.; O'Byrne, K. J. *J. Clin. Oncol.* **2003**, *21* (3), 473. (b) Wilkinson, B. L.; Bornaghi, L. F.; Houston, T. A.; Innocenti, A.; Vullo, D.; Supuran, C. T.; Poulsen, S. A. *J. Med. Chem.* **2007**, *50*, 1651.

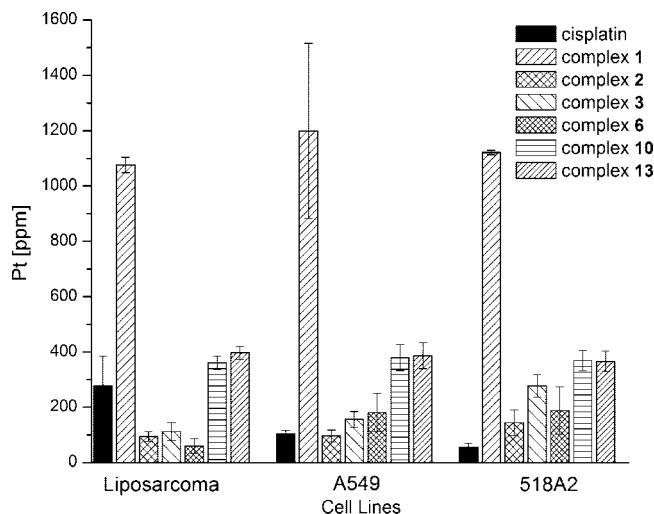


Figure 7. Platinum uptake (ppm) measured by atomic absorption spectroscopy (AAS) in lyophilized cells harvested after 24 h treatment with IC_{50} doses of the respective complex **1–3**, **6**, **10** and **13** or cisplatin on the cell lines liposarcoma, A549 and 518A2, respectively.

five ethyleneoxy groups (**3–6**) results in higher activity on the liposarcoma cell line only.

Changing the imidazol-1-yl moieties of **3** to benzimidazol-1-yl moieties (**10**) had a marginally negative effect on the activity toward A549 but otherwise did not influence the cytotoxicity. No major difference in activity was observed on any of the three tumor cell lines on going from the dibromo complex **3** to its diido derivative **13**. More extensive studies are required to determine the role of the ligands on the cytotoxicity of these complexes.

Drug uptake was determined by atomic absorption spectroscopy after 24 h exposure of the cell lines to the platinum complexes. The results are depicted in Figure 7. The uptake of **1** was substantially higher than for any of the other complexes but does not correlate to its activity, since it was not found to be the most or even as active as most of the other complexes tested. Otherwise the uptakes of **2**, **3** and **5** are similar and somewhat less than the uptake of **10** or **13** in each cell line. The activity cannot be correlated to the platinum uptake of the complexes in the three cell lines.

A study investigating the mode of cell death induced by **1–3**, **5**, **10** and **13**, respectively, showed that apoptosis (programmed cell death) is induced preferentially in all cell lines, as determined by a trypan blue staining test. Apoptotic cells with an intact cell membrane evince the ability to exclude the blue dye for a distinct time, whereas a breakdown of the cell membrane in necrotic cells leads to staining of the cells. Treatment of 518A2 with **1–3** and **6** respectively induced apoptosis after a short exposure time (12 h) and after a 24 h period a quick onset of secondary necrosis could be observed. Figure 8 illustrates images obtained of the three cell lines after a 24 h treatment with **3** (A–C) as well as after a 12 h treatment on 518A2 (D).

Summing up, new types of metallacrown ethers afforded in high yields via the reaction of α,ω -bis(imidazol-1-yl) or α,ω -bis(benzimidazol-1-yl) polyether-type ligands with a platinum(IV) precursor have been described. Investigations in weak donor solvents revealed that dialkylammonium ions can interact with such metallacrown ethers, as confirmed by the enhanced solubility of the dialkylammonium salts, NOE experiments and ESI-MS analysis. Furthermore these metallacrown ethers possess

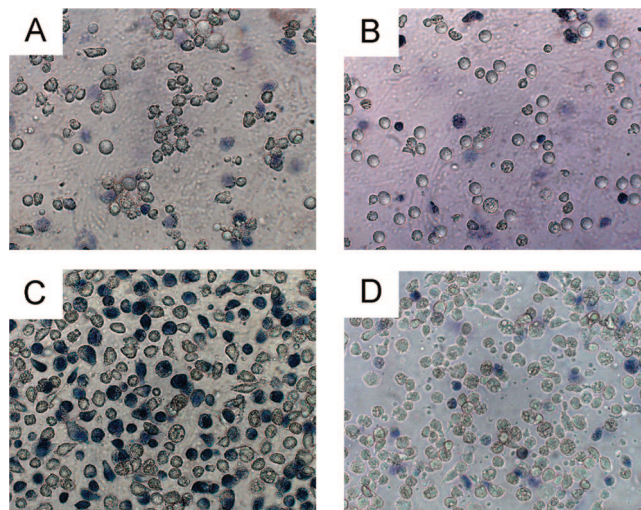


Figure 8. Images of floating cells obtained following a 24 h treatment of liposarcoma (A), A549 (B) and 518A2 (C) with **3** and of 518A2 after a 12 h treatment (D) with **3**. The ability of cells to exclude the dye indicates apoptosis. Stained cells in image C is concomitant with secondary necrosis. Image D shows the floating cells are not stained after a 12 h treatment.

significant *in vitro* antitumor activity. From our investigations on three chosen tumor cell lines it is in general found that the activity of the $PtBr_2Me_2$ moiety is enhanced by coordination to the polyether ligands.

3. Experimental Section

3.1. General Comments. All reactions were performed under an argon atmosphere using standard Schlenk techniques unless described otherwise. Solvents for the reactions were dried ($CHCl_3$ and CH_2Cl_2 over CaH_2) and distilled prior to use, except DMF (analytical grade, VWR), which was used as received. Purification by flash chromatography was performed using reagent grade solvents and silica gel 60 0.040–0.063 nm (Merck). 1H , ^{13}C and ^{195}Pt NMR spectra were recorded on Varian Gemini 2000 (200 and 400 MHz) and Varian Unity 500 (500 MHz) spectrometers. 1H and ^{13}C NMR chemical shifts are relative to solvent signals ($CDCl_3$ δ_H 7.24, δ_C 77.0; CD_2Cl_2 δ_H 5.32, δ_C 53.8; CD_3CN δ_H 1.93, δ_C 1.3; and $(CD_3)_2CO$ δ_H 2.04, δ_C 29.8). Assignment of NMR signals was partially revealed by COSY, HMBC and NOE experiments. ^{195}Pt NMR data were referenced to $H_2[PtCl_6]$ in D_2O (δ_{Pt} 0). IR spectra were recorded on a Galaxy Matteson 5000 FT-IR spectrometer using KBr pellets. Microanalyses were performed at the microanalytical laboratory at Martin-Luther-Universität Halle-Wittenberg using CHNS-932 (LECO) and Vario EL (Elementaranalysensysteme) elemental analyzers. High-resolution positive ion ESI-MS were obtained from a Bruker Apex III Fourier transform ion cyclotron resonance (FTICR) mass spectrometer (Bruker Daltonics, Billerica, MA) equipped with an Infinity cell, a 7.0 T superconducting magnet (Bruker, Karlsruhe, Germany), an rf-only hexapole ion guide and an external electrospray ion source (Agilent). Nitrogen was used as drying gas at 150 °C. The sample solutions were introduced continuously via a syringe pump with a flow rate of $120 \mu L h^{-1}$. The data were acquired with 512 k data points and zero filled to 2048 k by averaging 32 scans. $[(PtBr_2Me_2)_n]$ and $[PtMe_2(cod)]$ were prepared from $H_2[PtCl_6 \cdot 6H_2O]$ (Merck) by known procedures.^{15,24} The ammonium salts were synthesized according to a published procedure.^{20a} All ligands were prepared by modification of a procedure from the literature,³ although some

of the ligands have previously been obtained by various other means.²⁵ Ligands **L6**, **L7** and **L12** are prepared here for the first time according to the general procedure given. Heterocyclic rings are numbered according to IUPAC rules. C^e denotes all CH₂ groups of ethereal ethyleneoxy units not directly bound to a heterocyclic ring (these resonances are spectroscopically indistinguishable).

3.2. Synthesis of Ligands. To a flask fitted with a condenser the appropriate *N*-heterocycle (imidazole/benzimidazole) (28 mmol) and an excess of NaH (37 mmol) suspended in paraffin were added. At 0 °C under anaerobic conditions DMF (15 mL) was slowly added, and the reagents were stirred until no further H₂ evolved. A DMF solution (ca. 15 mL) of the appropriate glycol ditosylate (14 mmol) was added over 4–5 min and stirred for 15 min at ambient temperature before stirring at 82 °C for ca. 16 h. The reaction was then stopped and the solvent was removed under vacuum. The remaining residue was washed with ether (30 mL) and filtered. The residue was then partially dissolved in CH₂Cl₂ (100 mL) and filtered and the filtrate was evaporated to dryness to yield the crude product. The final product was obtained in satisfactory purity by flash chromatography.

3.2.1. imC⁶H₂C⁷H₂O(C⁶H₂C⁶H₂O)₄C⁷H₂C⁶H₂im (L6): flash chromatography: (a) ether/CH₂Cl₂ 20/80; (b) MeOH (final product). Transparent orange oil. Yield: 4.41 g (84%). ¹H NMR (400 MHz, CDCl₃): δ 3.57 (m, 16H, C⁶H₂), 3.70 (t, 4H, C⁷H₂), 4.06 (t, 4H, C⁶H₂), 6.95 (s, 2H, C⁵H₂), 6.99 (s, 2H, C⁴H₂), 7.49 (s, 2H, C²H). ¹³C NMR (101 MHz, CDCl₃): δ 47.0 (s, C⁶H₂), 70.4 (s, CH₂), 70.5 (s, CH₂), 70.6 (s, CH₂), 119.3 (s, C⁵H), 128.9 (s, C⁴H), 137.3 (s, C²H). EI-MS: [M]⁺⁺ calcd 382, found 382.

3.2.2. imC⁶H₂C⁷H₂O(C⁶H₂C⁶H₂O)₆C⁷H₂C⁶H₂im (L7): transparent yellow oil used without purification. Yield: 2.81 g (77%). ¹H NMR (400 MHz, CDCl₃): δ 3.58 (m, 24 H, C⁶H₂), 3.71 (t, 4H, C⁷H₂), 4.08 (t, 4H, C⁶H₂), 7.00 (s, 2H, C⁵H), 7.01 (s, 2H, C⁴H), 7.50 (s, 2H, C²H). ¹³C NMR (101 MHz, CDCl₃): δ 47.5 (s, C⁶H₂), 71.0 (s, CH₂), 71.2 (s, CH₂), 120.4 (s, C⁵H), 129.4 (s, C⁴H), 138.5 (s, C²H). EI-MS: [M]⁺⁺ calcd 470, found 470.

3.2.3. bimC⁸H₂C⁹H₂O(C⁶H₂C⁶H₂O)₆C⁹H₂C⁸H₂bim (L12): Purification by flash chromatography was preceded by precipitation from CH₂Cl₂/ether (1:10) and filtration to remove traces of unreacted sodium benimidazole. Flash chromatography: ether/MeOH (a) 95/5; (b) 90/10; (c) 0/100 (product). Transparent pale yellow oil. Yield: 1.35 g (45%). ¹H NMR (400 MHz, CDCl₃): δ 3.59 (m, 24 H, C⁶H₂), 3.81 (t, 4H, C⁹H₂), 4.31 (t, 4H, C⁸H₂), 7.26 (m, 4H, C^{5,6}H), 7.38 (m, 2H, C⁷H), 7.78 (m, 2H, C⁴H), 7.97 (s, 2H, C²H). ¹³C NMR (100 MHz, CDCl₃): δ 45.0 (s, C⁸H₂), 69.4 (s, C⁹H₂), 70.6 (m, C⁶H₂), 70.7 (s, C⁶H₂), 109.5 (s, C⁷H), 120.3 (s, C⁴H), 122.0 (s, C^{5,6}H), 122.8 (s, C^{5,6}H), 133.8 (s, C^{7a}), 143.7 (s, C²H, C^{3a}). EI-MS: [M]⁺⁺ calcd 570, found 570.

3.3. Synthesis of 1–13. Complexes **1–12** were prepared by analogy with a known procedure.¹¹ To a Schlenk vessel were added [(PtBr₂Me₂)_n] (69 mg, 0.18 mmol) and the appropriate bis(azol-1-yl) polyether/ethylene ligand (0.18 mmol). Under anaerobic conditions CHCl₃ (10 mL) was added. The reaction mixture was stirred for 24 h. For reactions yielding **1**, **2**, or **8** the product precipitated and was filtered off, washed with CHCl₃ (10 mL) and MeOH (20

mL), and dried under vacuum. Reaction mixtures yielding **3–7** and **9–12**, respectively, became transparent after stirring for 24 h, the solvent was removed under vacuum and the residue was treated as specified below.

3.3.1. [(PtBr₂Me₂)₂(μ-imC⁶H₂C⁶H₂im)₂] (1): light yellow powder. Yield: 37 mg (100%). T_{dec}: 154 °C. Anal. Calcd for C₂₀H₃₂Br₄N₈Pt₂ (1094.29): C, 21.87; H, 2.95; N, 10.24. Found: C, 21.69; H, 2.95; N, 10.24. ¹H NMR (400 MHz, (CD₃)₂CO): δ 1.76 (s+d, ²J_{Pt,H} = 71.0 Hz, 12H, CH₃), 4.69 (s, 8H, C⁶H₂), 6.85 (s, 4H, C⁵H), 7.21 (s(br), 4H, C⁴H), 8.08 (s(br), 4H, C²H). ¹³C NMR (125 MHz, (CD₃)₂CO): δ -10.9 (s, CH₃), 49.0 (s, C⁶H₂), 120.3 (s, C⁵H), 129.4 (s, C⁴H), 139.7 (s, C²H). ¹⁹⁵Pt NMR (107 MHz, (CD₃)₂CO): δ -2334 (s).

3.3.2. [(PtBr₂Me₂)₂(μ-imC⁶H₂C⁷H₂OC⁷H₂C⁶H₂im)₂] (2): light yellow powder. Yield: 53 mg (83%). T_{dec}: 71 °C. Anal. Calcd for C₂₄H₄₀Br₄N₈O₂Pt₂ (1182.40): C, 24.38; H, 3.41; N, 9.48. Found: C, 24.83; H, 3.73; N, 9.44. ¹H NMR (400 MHz, (CD₃)₂CO): δ 1.79 (s+d, ²J_{Pt,H} = 70.8 Hz, 12H, CH₃), 3.75 (t, 8H, C⁷H₂), 4.23 (t, 8H, C⁶H₂), 6.99 (s, 4H, C⁵H), 7.36 (s, 4H, C⁴H), 8.17 (s, 4H, C²H). ¹³C NMR (125 MHz, CD₃CN): δ -12.0 (s, CH₃), 48.3 (s, C⁶H₂), 69.5 (s, C⁷H₂), 120.4 (s, C⁵H), 129.1 (s, C⁴H), 142.3 (s, C²H). ¹⁹⁵Pt NMR (107 MHz, CD₃CN): δ -2326 (s).

3.3.3. [PtBr₂Me₂(imC⁶H₂C⁷H₂OC⁸H₂C⁸H₂OC⁷H₂C⁶H₂im)] (3): yellow microcrystalline solid from CHCl₃/pentane (1:10). Yield: 89 mg (95%). T_{dec}: 143 °C. ¹H NMR (400 MHz, CDCl₃): δ 1.91 (s+d, ²J_{Pt,H} = 70.6 Hz, 6H, CH₃), 3.46 (s, 4H, C⁸H₂), 3.58 (t, 4H, C⁷H₂), 4.04 (t, 4H, C⁶H₂), 6.84 (s, 2H, C⁵H), 7.55 (s, 2H, C⁴H), 7.87 (s, 2H, C²H). ¹³C NMR (125 MHz, CDCl₃): δ -10.5 (s+d, ¹J_{Pt,C} = 506.0 Hz, CH₃), 48.1 (s, C⁶H₂), 69.2 (s, C⁷H₂), 70.1 (s, C⁸H₂), 118.9 (s, C⁵H), 128.2 (s, C⁴H), 139.9 (s, C²H). ¹⁹⁵Pt NMR (107 MHz, CDCl₃): δ -2362 (s). Positive ion ESI-FTICR-MS (MeOH): *m/z* 710.90922 [3+Br]⁺, calcd for [C₁₄H₂₄⁷⁹Br₂N₄O₂¹⁹⁴Pt+Br]⁺ 710.90815.

3.3.4. [PtBr₂Me₂(imC⁶H₂C⁷H₂O(C⁶H₂C⁶H₂O)₂C⁷H₂C⁶H₂im)] (4): yellow microcrystalline solid from CHCl₃/pentane (1:10). Yield: 89 mg (95%). T_{dec}: 100 °C. Anal. Calcd for C₁₆H₂₈Br₂N₄O₃Pt (679.30): C, 28.29; H, 4.15; N, 8.25. Found: C, 29.30; H, 4.41; N, 8.09. ¹H NMR (400 MHz, CDCl₃): δ 1.88 (s+d, ²J_{Pt,H} = 70.6 Hz, 6H, CH₃), 3.55 (m, 8H, C⁶H₂), 3.69 (t, 4H, C⁷H₂), 4.07 (t, 4H, C⁶H₂), 6.85 (s, 2H, C⁵H), 7.49 (s(br), 2H, C⁴H), 8.09 (s(br), 2H, C²H). ¹³C NMR (125 MHz, CDCl₃): δ -10.6 (s+d, ¹J_{Pt,C} = 504.5 Hz, CH₃), 48.2 (s, C⁶H₂), 69.5 (s, C⁷H₂), 70.8 (s, C⁶H₂), 71.4 (s, C⁶H₂), 119.7 (s, C⁵H), 128.0 (s, C⁴H), 139.2 (s, C²H). ¹⁹⁵Pt NMR (107 MHz, CDCl₃): δ -2361 (s). Positive ion ESI-FTICR-MS (MeOH): *m/z* 754.93539 [4+Br]⁺, calcd for [C₁₆H₂₈⁷⁹Br₂N₄O₃¹⁹⁴Pt+Br]⁺ 754.93437.

3.3.5. [PtBr₂Me₂(imC⁶H₂C⁷H₂O(C⁶H₂C⁶H₂O)₃C⁷H₂C⁶H₂im)] (5): light yellow microcrystalline solid from CHCl₃/pentane (1:10). Yield: 49 mg (88%). T_{dec}: 143 °C. Anal. Calcd for C₁₈H₃₂Br₂N₄O₄Pt (723.36): C, 29.89; H, 4.46; N, 7.75. Found: C, 30.31; H, 4.84; N, 7.65. ¹H NMR (400 MHz, CDCl₃): δ 1.89 (s+d, ²J_{Pt,H} = 70.6 Hz, 6H, CH₃), 3.56 (m, 12H, C⁶H₂), 3.70 (t, 4H, C⁷H₂), 4.07 (t, 4H, C⁶H₂), 7.01 (s, 2H, C⁵H), 7.24 (s, 2H, C⁴H), 8.05 (s, 2H, C²H). ¹³C NMR (125 MHz, CDCl₃): δ -10.5 (s+d, ¹J_{Pt,C} = 506.3 Hz, CH₃), 48.1 (s, C⁶H₂), 69.8 (s, C⁷H₂), 70.5 (s, C⁶H₂), 70.9 (s, C⁶H₂), 70.9 (s, C⁶H₂), 119.9 (s, C⁵H), 128.3 (s, C⁴H), 138.9 (s, C²H). ¹⁹⁵Pt NMR (107 MHz, CDCl₃): δ -2356 (s). Positive mode ESI-FTICR-MS (CH₂Cl₂/MeOH, 1:10): *m/z* 743.03046 [5+Na]⁺, calcd for [C₁₈H₃₂⁷⁹Br₂N₄O₄¹⁹⁴Pt+Na]⁺ 743.03092.

3.3.6. [PtBr₂Me₂(imC⁶H₂C⁷H₂O(C⁶H₂C⁶H₂O)₄C⁷H₂C⁶H₂im)] (6): viscous yellow residue. Yield: 55 mg (72%). Anal. Calcd for C₂₀H₃₆Br₂N₄O₅Pt (767.41): C, 31.30; H, 4.73; N, 7.30. Found: C, 31.13; H, 4.99; N, 7.12. ¹H NMR (400 MHz, CDCl₃): δ 1.91 (s+d, ²J_{Pt,H} = 70.8 Hz, 6H, CH₃), 3.61 (m, 16H, C⁶H₂), 3.73 (t, 4H, C⁷H₂), 4.08 (t, 4H, C⁶H₂), 7.04 (s, 2H, C⁵H), 7.43 (s, 2H, C⁴H), 8.08 (s, 2H, C²H). ¹³C NMR (125 MHz, CDCl₃): δ -10.6 (s+d, ¹J_{Pt,C} = 504.3 Hz, CH₃), 48.0 (s, C⁶H₂), 69.9 (s, C⁷H₂), 70.6 (s,

(25) (a) Cabildo, P.; Claramunt, R. M.; Cornago, P.; Lavandera, J. L.; Sanz, D.; Jagerovic, N.; Jimeno, M. L.; Elguero, J.; Gilles, I.; Aubagnac, J. L. *J. Chem. Soc., Perkin Trans. 2* **1996**, 701. (b) Wu, L. P.; Yamagiwa, Y.; Kuroda-Sowa, T.; Kamikawa, T.; Munakata, M. *Inorg. Chim. Acta* **1997**, 256, 155. (c) Meth-Cohn, O.; Smith, D. I. *J. Chem. Soc., Perkin Trans. 1* **1982**, 261. (d) Hausner, S. H.; Striley, C. A. F.; Krauser-Bauer, J. A.; Zimmer, H. *J. Org. Chem.* **2005**, 70, 5804. (e) Bitter, I.; Török, Z.; Csokai, V.; Grün, A.; Balázs, B.; Tóth, G.; Keserü, G. M.; Kovári, Z.; Czugler, M. *Eur. J. Org. Chem.* **2001**, 2861. (f) Lavandera, J. L.; Cabildo, P.; Claramunt, R. M. *J. Heterocycl. Chem.* **1988**, 25 (3), 771. (g) Díez-Barra, E.; de la Hoz, A.; Sánchez-Migallón, A.; Tejada, J. *Heterocycles* **1992**, 34 (7), 1365. (h) Hull, R.; Hollywood, F.; Suschitzky, H. *J. Chem. Soc., Perkin Trans. 1* **1979**, 3037. (i) Park, S. H.; Demberlymba, D.; Jang, S. H.; Byun, M. W. *Chem. Lett.* **2006**, 35 (9), 1024. (j) Zhou, C.-H.; Gu, X.-R.; Xie, R.-G.; Cai, M.-S. *Synth. Commun.* **1999**, 29 (7), 1217.

C^6H_2), 70.7 (s, C^6H_2), 70.8 (s, C^6H_2) 120.0 (s, C^5H), 128.3 (s, C^4H), 138.7 (s, C^2H). ^{195}Pt NMR (107 MHz, $CDCl_3$): δ -2360 (s). Positive mode ESI-FTICR-MS ($CH_2Cl_2/MeOH$, 1:10): m/z 787.05931 $[6+Na]^+$, calcd for $[C_{20}H_{36}^{79}Br_2N_4O_5^{194}Pt+Na]^+$ 787.05713.

3.3.7. $[PtBr_2Me_2\{imC^6H_2C^7H_2O(C^6H_2C^6H_2O)_6C^7H_2C^6H_2im\}]$ (7): viscous orange residue. Crude yield: 240 mg (100%). Anal. Calcd for $C_{24}H_{44}Br_2N_4O_7Pt$ (855.51): C, 33.69; H, 5.18; N, 6.55. Found: C, 33.03; H, 5.20; N, 6.05. 1H NMR (400 MHz, $CDCl_3$): δ 1.88 (s+d, $^2J_{Pt,H} = 70.6$ Hz, 6H, CH_3), 3.57 (m, 24H, C^6H_2), 3.72 (t, 4H, C^7H), 4.08 (t, 4H, C^6H_2), 7.01 (s, 2H, C^5H), 7.43 (s, 2H, C^4H), 8.04 (s(br), 2H, C^2H). ^{13}C NMR (125 MHz, $CDCl_3$): δ -10.7 (s+d, $^1J_{Pt,C} = 504.1$ Hz, CH_3), 47.9 (s, C^6H_2), 69.9 (s, C^7H), 70.6 (m, C^6H_2), 120.0 (s, C^5H), 128.1 (s, C^4H), 138.7 (s, C^2H). ^{195}Pt NMR (107 MHz, $CDCl_3$): δ -2356 (s). Positive mode ESI-FTICR-MS ($CH_2Cl_2/MeOH$, 1:10): m/z 875.10692 $[7+Na]^+$, calcd for $[C_{24}H_{44}^{79}Br_2N_4O_7^{194}Pt+Na]^+$ 875.10956.

3.3.8. $[(PtBr_2Me_2)_2(\mu-bimCH_2CH_2bim)_2]$ (8): yellow powder filtered from the reaction mixture. Yield: 29 mg (100%). T_{dec} : 121 °C. Anal. Calcd for $C_{36}H_{44}Br_4N_8Pt_2$ (1294.52): C, 33.40; H, 3.11; N, 8.66. Found: C, 33.45; H, 3.62; N, 8.27.

3.3.9. $[PtBr_2Me_2(bimC^8H_2C^9H_2OC^9H_2C^8H_2bim)]$ (9): bright yellow microcrystalline solid from CH_2Cl_2 /pentane (1:10). Yield: 114 mg (97%). T_{dec} : 138 °C. Anal. Calcd for $C_{20}H_{24}Br_2N_4OPt$ (691.32): C, 34.75; H, 3.50; N, 8.10. Found: C, 35.06; H, 3.56; N, 8.08. 1H NMR (400 MHz, CD_2Cl_2): δ 2.40 (s+d, $^2J_{Pt,H} = 73.5$ Hz, 6H, CH_3), 3.71 (t, 4H, C^9H_2), 4.23 (t, 4H, C^8H_2), 7.38 (m, 4H, C^5-6H), 7.48 (m, 2H, C^7H), 7.53 (s+d, $^3J_{Pt,H} = 5.8$ Hz, 2H, C^2H), 8.36 (m, 2H, C^4H). ^{13}C NMR (50 MHz, CD_2Cl_2): δ -9.9 (s, CH_3), 45.2 (s, C^8H_2), 66.7 (s, C^9H_2), 110.5 (s, C^7H), 121.8 (s, C^4H), 123.2 (s, $C^5/6H$), 124.0 (s, $C^5/6H$), 133.5 (s, C^7a), 148.7 (s, C^2H). ^{195}Pt NMR (107 MHz, CD_2Cl_2): δ -2324 (s).

3.3.10. $[PtBr_2Me_2(bimC^8H_2C^9H_2OC^{10}H_2C^{10}H_2OC^9H_2C^8H_2bim)]$ (10): yellow microcrystalline solid from CH_2Cl_2 /pentane (1:10). Yield: 210 mg (83%). T_{dec} : 94 °C. Anal. Calcd for $C_{22}H_{28}Br_2N_4O_2Pt \cdot CHCl_3$ (735.37): C, 32.32; H, 3.42; N, 6.55. Found: C, 32.33; H, 3.92; N, 6.23. 1H NMR (400 MHz, CD_2Cl_2): δ 2.16 (s+d, $^2J_{Pt,H} = 72.2$ Hz, 6H, CH_3), 3.40 (s, 4H, $C^{10}H_2$), 3.67 (t, 4H, C^9H_2), 4.32 (t, 4H, C^8H_2), 7.38 (m, 4H, C^5-6H), 7.48 (m, 2H, C^7H), 8.26 (s+d, $^3J_{Pt,H} = 6.9$ Hz, 2H, C^2H), 8.53 (m, 2H, C^4H). ^{13}C NMR (125 MHz, CD_2Cl_2): δ -8.6 (s+d, $^1J_{Pt,C} = 516.4$ Hz, CH_3), 46.4 (s, C^8H_2), 70.0 (s, C^9H_2), 70.4 (s, $C^{10}H_2$), 110.5 (s, C^7H), 121.8 (s, C^4H), 123.2 (s, C^5H), 124.0 (s, C^6H), 133.5 (s, C^7a), 140.0 (s, C^3a), 148.7 (s, C^2H). ^{195}Pt NMR (107 MHz, CD_2Cl_2): δ -2306 (s).

3.3.11. $[PtBr_2Me_2\{bimC^8H_2C^9H_2O(C^6H_2C^6H_2O)_4C^9H_2C^8H_2bim\}]$ (11): yellow powder from CH_2Cl_2 /pentane (1:10) at -18 °C. Yield: 133 mg (82%). T_{dec} : 131 °C. Anal. Calcd for $C_{28}H_{40}Br_2N_4O_3Pt$ (867.53): C, 38.77; H, 4.65; N, 6.46. Found: C, 38.88; H, 4.81; N, 6.53. 1H NMR (400 MHz, $CDCl_3$): δ 2.25 (s+d, $^2J_{Pt,H} = 71.8$ Hz, 6H, CH_3), 3.51 (m, 16H, C^6H_2), 3.69 (t, 4H, C^9H_2), 4.29 (t, 4H, C^8H_2), 7.17 (m, 2H, C^5H), 7.28 (m, 2H, C^6H), 7.40 (d, $^3J_{H,H} = 8.1$ Hz, 2H, C^7H), 8.00 (d, $^3J_{H,H} = 8.3$ Hz, 2H, C^4H), 8.26 (s+d, $^3J_{Pt,H} = 7.3$ Hz, 2H, C^2H). ^{13}C NMR (125 MHz, $CDCl_3$): δ -8.3 (s+d, $^1J_{Pt,C} = 513.9$ Hz, CH_3), 45.4 (s, C^8H_2), 69.1 (s, C^9H_2), 70.3 (s, C^6H_2), 70.5 (s, C^6H_2), 70.7 (s, CH_2), 71.0 (s, C^6H_2), 110.0 (s, C^7H), 121.2 (s, C^4H), 122.9 (s, C^5H), 123.5 (s, C^6H), 133.5 (s, C^7a), 139.9 (s, C^3a), 146.9 (s, C^2H). ^{195}Pt NMR (107 MHz, $CDCl_3$): δ -2338 (s). Positive mode ESI-FTICR-MS ($CH_2Cl_2/MeOH$, 1:10): m/z 887.08915 $[11+Na]^+$, calcd for $[C_{28}H_{40}^{79}Br_2N_4O_3^{194}Pt+Na]^+$ 887.08843.

3.3.12. $[PtBr_2Me_2\{bimC^8H_2C^9H_2O(C^6H_2C^6H_2O)_6C^9H_2C^8H_2bim\}]$ (12): viscous yellow oil. Yield: 107 mg (100%). 1H NMR (400 MHz, CD_2Cl_2): δ 2.17 (s+d, $^2J_{Pt,H} = 71.6$ Hz, 6H, CH_3), 3.52 (m, 24H, C^6H_2), 3.72 (t, 4H, C^9H_2), 4.33 (t, 4H, C^8H_2), 7.13 (m, 2H, C^5H), 7.31 (m, 2H, C^6H), 7.50 (d, $^3J_{H,H} = 8.1$ Hz, 2H, C^7H), 7.85 (d, $^3J_{H,H} = 8.3$ Hz, 2H, C^4H), 8.26 (s+d, $^3J_{Pt,H} = 7.7$ Hz, 2H, C^2H). ^{13}C NMR (100 MHz, CD_2Cl_2): δ -8.1 (s+d, $^1J_{Pt,C}$

= 515.0 Hz, CH_3), 46.1 (s, C^8H_2), 69.4 (s, C^9H_2), 70.2 (s, C^6H_2), 71.0 (m, C^6H_2), 110.8 (s, C^7H), 121.2 (s, C^4H), 122.8 (s, C^5H), 123.7 (s, C^6H), 133.9 (s, C^7a), 140.2 (s, C^3a), 147.1 (s, C^2H). ^{195}Pt NMR (107 MHz, CD_2Cl_2): δ -2328 (s). Positive ion ESI-FTICR-MS ($CH_2Cl_2/MeOH/MeCN$, 2:2:1): m/z 953.15917 $[12+H]^+$, calcd for $[C_{32}H_{48}^{79}Br_2N_4O_7^{194}Pt+H]^+$ 953.15892.

3.3.13. $[PtH_2Me_2\{imC^6H_2C^7H_2OC^6H_2C^8H_2OC^7H_2C^6H_2im\}]$ (13): The procedure is a modification of a previously described one,¹⁴ differing only in isolation of the desired complex: decantation and recrystallization were repeated a number of times and yielded the product as a dark orange powder. Yield: 130 mg (75%). T_{dec} : 125 °C. Anal. Calcd for $C_{14}H_{24}I_2N_4O_2Pt$ (729.25): C, 23.06; H, 3.32; N, 7.68. Found: C, 23.52; H, 3.91; N, 7.45. 1H NMR (400 MHz, $CDCl_3$): δ 2.32 (s+d, $^2J_{Pt,H} = 72.6$ Hz, 6H, CH_3), 3.48 (s, 4H, C^8H_2), 3.58 (t, 4H, C^7H), 4.05 (t, 4H, C^6H_2), 6.82 (s, 2H, C^5H), 7.65 (s(br), 2H, C^4H), 7.92 (s, 2H, C^2H). ^{13}C NMR (100 MHz, $CDCl_3$): δ -19.3 (s, CH_3), 48.2 (s, C^6H_2), 69.3 (s, C^7H_2), 70.1 (s, C^8H_2), 106.3 (s, C^5H), 130.6 (s, C^4H), 142.5 (s, C^2H). ^{195}Pt NMR (107 MHz, $(CD_3)_2CO$): δ -2738 (s).

3.4. Host-Guest Studies. The appropriate ligand (**L5-L7; L12**) (0.07 mmol) $[(PtBr_2Me_2)_n]$ (27 mg, 0.07 mmol) and the relevant ammonium hexafluorophosphate (0.07 mmol) were added to an NMR tube. CD_2Cl_2 (0.75 mL) was then added. The tube was sealed and allowed to shake for approximately 24 h before performing NMR experiments. The same scale of reaction was performed in parallel in a flask using commercially available CH_2Cl_2 . This reaction mixture was filtered after 24 h, the filtrate was evaporated and the remaining oily residue was diluted accordingly for ESI-FTICR-MS analysis. Variations of this procedure are specified below.

3.4.1. Reaction of $[(PtBr_2Me_2)_n]/L5$ ($\rightarrow 5$) with $[Bn_2NH_2][PF_6]$. 1H NMR (400 MHz, CD_2Cl_2): δ 1.83 (s+d, $^2J_{Pt,H} = 70.6$ Hz, 6H, CH_3), 3.56 (m, 12H, C^6H_2), 3.72 (m, 4H, C^7H_2), 4.10 (m, 4H, C^6H_2), 4.17 (s, 2H, Ph- CH_2),²⁶ 7.07 (s, 2H, C^5H), 7.39 (s(br), 2H, C^4H), 7.42 (s, 5H, Ph- H), 8.05 (s(br), 2H, C^2H). ^{13}C NMR (101 MHz, CD_2Cl_2): δ -10.7 (s+d, $^1J_{Pt,C} = 508.3$ Hz, CH_3), 48.4 (s, C^6H_2), 51.3 (s, Ph- CH_2), 70.1 (s, C^7H), 70.9 (m, C^6H_2), 120.3 (s, C^5H), 128.3 (s, C^4H), 129.8 (s, *o*m- CH , Ph), 130.0 (s, *i*- C , Ph), 130.3 (s, *o*m- CH , Ph), 130.4 (s, *p*- CH , Ph), 139.4 (s, C^2H). ^{195}Pt NMR (107 MHz, CD_2Cl_2): δ -2345 (s(br)). Positive mode ESI-FTICR-MS ($CH_2Cl_2/MeOH$, 1:10): m/z 918.16835 $[5+Bn_2NH_2]^+$, calcd for $[C_{18}H_{32}^{79}Br_2N_4O_4^{194}Pt+Bn_2NH_2]^+$ 918.16942.

3.4.2. Reaction of $[(PtBr_2Me_2)_n]/L5$ ($\rightarrow 5$) with $[(CH_3C^7H_2-C^6H_2C^6H_2)_2NH_2][PF_6]$. 1H NMR (400 MHz, CD_2Cl_2): δ 0.94 (t, $^3J_{H,H} = 7.3$ Hz, 6H, $C^7H_2CH_3$), 1.38 (m, 4H, C^7H_2), 1.68 (m, 4H, C^6H_2), 1.83 (s+d, $^2J_{Pt,H} = 70.6$ Hz, 6H, $PtCH_3$), 2.99 (s(br), 4H, C^6H_2), 3.56 (m, 12H, C^6H_2), 3.74 (m, 4H, C^7H_2), 4.20 (m, 4H, C^6H_2), 6.94 (s(br), NH_2), 7.07 (m, 2H, C^5H), 7.39 (s(br), 2H, C^4H), 8.06 (s(br), 2H, C^2H). ^{13}C NMR (101 MHz, CD_2Cl_2): δ -10.7 (s+d, $^1J_{Pt,C} = 507.3$ Hz, CH_3), 13.6 (s, $C^7H_2CH_3$), 20.0 (s, C^7H_2), 28.2 (s, C^6H_2), 48.5 (s, C^6H_2), 48.9 (s, C^6H_2), 70.1 (s, C^7H), 71.0 (m, C^6H_2), 120.0 (s, C^5H), 128.2 (s, C^4H), 138.5 (s, C^2H). ^{195}Pt NMR (107 MHz, CD_2Cl_2): δ -2339 (s(br)). Positive mode ESI-FTICR-MS ($CH_2Cl_2/MeOH$, 1:10): m/z 850.20197 $[5+Bu_2NH_2]^+$, calcd for $[C_{18}H_{32}^{79}Br_2N_4O_4^{194}Pt+Bu_2NH_2]^+$ 850.20072.

3.4.3. Reaction of $[(PtBr_2Me_2)_n]/L6$ ($\rightarrow 6$) with $[Bn_2NH_2][PF_6]$. 1H NMR (400 MHz, CD_2Cl_2): δ 1.82 (s+d, $^2J_{Pt,H} = 70.6$ Hz, 6H, CH_3), 3.75 (m, 28H, $C^{6,7}H_2$, Ph- CH_2), 6.99 (s, 2H, C^5H), 7.38 (m, 10.8H, C^4H , Ph- H), 7.51 (s, 1.2H, C^4H), 8.02 (m(br), 0.8H, C^2H), 8.16 (s(br), 1.2H, C^2H). ^{13}C NMR (101 MHz, CD_2Cl_2): δ -10.7 (s, CH_3), 47.8 (s, C^6H_2), 51.7 (s, Ph- CH_2), 69.5 (s, C^7H), 70.0 (m, C^6H_2), 120.3 (s(br), C^5H), 128.3 (s, (br) C^4H), 129.1 (s,

(26) Number of protons based on relative intensity ratio ammonium ion: metallacrown ether.

(27) (a) IPDS-Software package, Stoe & Cie, 1999. (b) SCALE3 ABSPACK: Empirical absorption correction; CrysAlis Software Package; Oxford Diffraction Ltd., 2006.

Table 4. Crystallographic and Data Collection Parameters for 2·2THF, 3·CHCl₃ and 5

	2·2THF	3·CHCl ₃	5
empirical formula	C ₃₂ H ₅₆ Br ₄ N ₈ O ₄ Pt ₂	C ₁₅ H ₂₅ Br ₂ Cl ₃ N ₄ O ₂ Pt	C ₁₈ H ₃₂ Br ₂ N ₄ O ₄ Pt
<i>M_r</i>	1326.67	754.65	723.39
cryst syst	triclinic	triclinic	monoclinic
space group	<i>P</i> $\bar{1}$	<i>P</i> $\bar{1}$	<i>P</i> ₂ / <i>c</i>
<i>a</i> /Å	8.669(2)	10.438(3)	11.9689(2)
<i>b</i> /Å	11.457(3)	10.449(2)	25.0784(4)
<i>c</i> /Å	12.083(3)	11.270(3)	8.1507(1)
α /deg	110.14(3)	103.19(3)	90
β /deg	91.04(3)	93.43(3)	105.143(2)
γ /deg	105.57(3)	94.59(3)	90
<i>V</i> /Å ³	1077.3(4)	1189.0(5)	2361.57(6)
<i>Z</i>	1	2	4
<i>D</i> _{calcd} /g·cm ⁻³	2.045	2.108	2.035
<i>T</i> /K	220(2)	220(2)	130(2)
μ (Mo K α)/mm ⁻¹	10.238	9.616	9.356
<i>F</i> (000)	632	716	1392
θ range/deg	1.98–25.94	2.60–25.96	2.71–30.03
no. of rflns collected	8061	9328	67973
no. of indep rflns	3839	4291	6909
no. data/restr/params	3839/0/228	4291/0/246	6909/0/264
goodness-of-fit <i>F</i> ²	1.047	1.043	0.928
<i>R</i> ₁ , <i>wR</i> ₂ (<i>I</i> > 2 σ (<i>I</i>))	0.0421, 0.1048	0.0250, 0.0657	0.0276, 0.0385
<i>R</i> ₁ (all data)	0.0541, 0.1189	0.0312, 0.0732	0.0619, 0.0469
largest diff peak and hole/e·Å ⁻³	1.462, -1.416	1.137, -1.598	1.941, -0.961
<i>T</i> _{min} / <i>T</i> _{max}	0.241/0.522	0.198/0.408	0.489/1.000

olm-CH, Ph), 129.7 (s, *i*-C, Ph), 129.8 (s, *olm*-CH, Ph), 130.5 (s, *p*-CH, Ph), 138.7 (m, C²H). ¹⁹⁵Pt NMR (107 MHz, CD₂Cl₂): δ -2341 (m(br)). Positive mode ESI-FTICR-MS (CH₂Cl₂/MeOH, 1:10): *m/z* 962.19620 [6+Bn₂NH₂]⁺, calcd for [C₂₀H₃₆⁷⁹Br₂N₄O₅¹⁹⁴Pt+Bn₂NH₂]⁺ 962.19564.

3.4.4. Reaction of [(PtBr₂Me₂)_n]/L6 (→6) with [Bu₂NH₂][PF₆]. ¹H NMR (400 MHz, CD₂Cl₂): δ 0.92 (t, 6H, ³*J*_{H,H} = 7.3 Hz, C^γH₂CH₃), 1.35 (m, 4H, C^γH₂), 1.63 (m, 4H, C^βH₂), 1.81 (s+d, ²*J*_{Pt,H} = 70.8 Hz, 6H, PtCH₃), 2.84 (m, 4H, C^αH₂), 3.58 (m, 16H, C^εH₂), 3.75 (m, 4H, C⁷H₂), 4.12 (m, 4H, C⁶H₂), 7.03 (s(br), 1H, C⁵H), 7.06 (s, 1H, C⁵H), 7.37 (s(br), 1H, C⁴H), 7.48 (s, 1H, C⁴H), 8.04 (s(br), 1H, C²H), 8.11 (s, 1H, C²H). ¹³C NMR (101 MHz, CD₂Cl₂): δ -10.5 (s+d, ¹*J*_{Pt,C} = 506.9 Hz, CH₃), 13.7 (s, C^γH₂CH₃), 20.1 (s, C^γH₂), 28.3 (s, C^βH₂), 48.3 (s, C⁶H₂), 48.8 (s, C^αH₂), 70.1 (s, CH₂), 70.2 (s, CH₂), 70.9 (m, CH₂), 120.4 (m, C⁵H), 128.3 (s, C⁴H), 139.0 (m, C²H). ¹⁹⁵Pt NMR (107 MHz, CD₂Cl₂): δ -2338 (s), -2345 (s). Positive mode ESI-FTICR-MS (CH₂Cl₂/MeOH, 1:10): *m/z* 894.22524 [6+Bu₂NH₂]⁺, calcd for [C₂₀H₃₆⁷⁹Br₂N₄O₅¹⁹⁴Pt+Bu₂NH₂]⁺ 894.22694.

3.4.5. Reaction of [(PtBr₂Me₂)_n]/L7 (→7) with [Bu₂NH₂][PF₆]. ¹H NMR (400 MHz, CD₂Cl₂): δ 1.83 (s+d, ²*J*_{Pt,H} = 70.6 Hz, 6H, CH₃), 3.23 (m, 4H, CH₂), 3.39 (m, 4H, CH₂), 3.60 (m, 20H, CH₂), 3.99 (m, 4H, C⁶H₂), 4.17 (s, Ph-CH₂), 4.60 (s(br), 2H, NH₂), 6.95 (m, 2H, C⁵H), 7.44 (m, 12H, C⁴H, Ph-H), 8.01 (s(br), 2H, C²H). ¹³C NMR (101 MHz, CD₂Cl₂): δ -10.6 (s, CH₃), 48.1 (s, C⁶H₂), 52.2 (s, Ph-CH₂), 69.8 (s, C⁷H), 70.5 (m, C^εH₂), 120.3 (s(br), C⁵H), 128.3 (s, C⁴H), 129.3 (s, *olm*-CH, Ph), 129.9 (s, *p*-C, Ph), 130.3 (s, *olm*-CH, Ph), 131.5 (s, *i*-CH, Ph), 139.3 (m, C²H). ¹⁹⁵Pt NMR (107 MHz, CD₂Cl₂): δ -2342 (m(br)). Positive mode ESI-FTICR-MS (CH₂Cl₂/MeOH, 1:10): *m/z* 1050.25490 [7+Bn₂NH₂]⁺, calcd for [C₂₄H₄₄⁷⁹Br₂N₄O₇¹⁹⁴Pt+Bn₂NH₂]⁺ 1050.24806.

3.4.6. Reaction of [(PtBr₂Me₂)_n]/L7 (→7) with [Bu₂NH₂][PF₆]. ¹H NMR (400 MHz, CD₂Cl₂): δ 0.94 (t, ³*J*_{H,H} = 7.4 Hz, 6H, C^γH₂CH₃), 1.38 (m, 4H, C^γH₂), 1.65 (m, 4H, C^βH₂), 1.81 (s+d, ²*J*_{Pt,H} = 70.6 Hz, 1.8H, PtCH₃), 1.84 (s+d, ²*J*_{Pt,H} = 70.6 Hz, 4.2H, PtCH₃), 2.98 (s(br), 4H, C^αH₂), 3.63 (m, 12H, C^εH₂), 3.74 (m, 4H, C⁷H₂), 4.11 (m, 4H, C⁶H₂), 7.03 (m, 2H, C⁵H), 7.13 (s(br), 2H, NH₂), 7.38 (s, 0.8H, C⁴H), 7.41 (m, 1.2H, C⁴H), 8.06 (s(br), 2H, C²H). ¹³C NMR (101 MHz, CD₂Cl₂): δ -10.7 (s, CH₃), 13.8 (s, C^γH₂CH₃), 20.1 (s, C^γH₂), 28.6 (s, C^βH₂), 48.4 (s, C⁶H₂), 49.0 (s, C^αH₂), 70.1 (s, CH₂), 70.2 (s, CH₂), 70.9 (m, CH₂), 120.3 (s, C⁵H), 128.4 (s, C⁴H), 139.4 (s, C²H). ¹⁹⁵Pt NMR (107 MHz, CD₂Cl₂): δ

-2339 (s), -2339 (s). Positive mode ESI-FTICR-MS (CH₂Cl₂/MeOH, 1:10): *m/z* 982.28148 [7+Bu₂NH₂]⁺, calcd for [C₂₄H₄₄⁷⁹Br₂N₄O₇¹⁹⁴Pt+Bu₂NH₂]⁺ 982.27937.

3.4.7. Reaction of [PtBr₂Me₂{bimC⁸H₂C⁹H₂O(C^εH₂C^εH₂O)₄-C⁹H₂C⁸H₂bim} (11) with [Bu₂NH₂][PF₆]. As per the general procedure, except **11** (51 mg, 0.07 mmol) was combined directly with [Bu₂NH₂][PF₆] instead of **L11** and [(PtBr₂Me₂)_n]. ¹H NMR (400 MHz, CDCl₃): δ 2.20 (s+d, ²*J*_{Pt,H} = 70.6 Hz, 6H, CH₃), 3.60 (m(br), 16H, C⁹H₂), 3.70 (t, 4H, C⁹H₂), 4.10 (s(br), 2H, Ph-CH₂), 4.28 (t, 4H, C⁸H₂), 7.20 (m, 2H, C⁵H), 7.30 (m, 2H, C⁶H), 7.39 (m, 2H, 5H, C⁷H₂, Ph-H), 8.00 (d, ³*J*_{H,H} = 8.0 Hz, 2H, C⁴H₂), 8.33 (s(br), 2H, C²H). ¹³C NMR (125 MHz, CD₂Cl₂): δ -4.0 (PtCH₃), 45.9 (s, C⁸H₂), 51.7 (s, Ph-CH₂), 69.6 (s, C⁹H₂), 70.6 (s, C^εH₂), 70.9 (s, C^εH₂), 71.0 (s, C^εH₂), 71.2 (s, C^εH₂), 111.0 (s, C⁷H), 121.6 (s, C⁴H), 123.4 (s(br), C⁵H), 124.3 (s(br), C⁶H), 129.9 (s, *olm*-CH, Ph), 130.2 (s, *i*-C, Ph), 130.5 (s, *olm*-CH, Ph), 130.6 (s, *p*-CH, Ph), 134.1 (s, C^{7a}), 140.4 (s, C^{3a}), 147.5 (s(br), C²H). ¹⁹⁵Pt NMR (107 MHz, CD₂Cl₂): δ -2322 (s). Positive mode ESI-FTICR-MS (CH₂Cl₂/MeOH, 1:10): *m/z* 1062.22925 [11+Bu₂NH₂]⁺, calcd for [C₂₈H₄₀⁷⁹Br₂N₄O₅¹⁹⁴Pt+Bu₂NH₂]⁺ 1062.22693.

3.4.8. Reaction of [PtBr₂Me₂{bimC⁸H₂C⁹H₂O(C^εH₂C^εH₂O)₄-C⁹H₂C⁸H₂bim} (11) with [Bu₂NH₂][PF₆]. As per the general procedure, except **11** (51 mg, 0.07 mmol) was combined directly with [Bu₂NH₂][PF₆] instead of **L11** and [(PtBr₂Me₂)_n]. ¹H NMR (400 MHz, CD₂Cl₂): δ 0.93 (t, ³*J*_{H,H} = 7.4 Hz, 6H, C^γH₂CH₃), 1.35 (m, 4H, C^γH₂), 1.68 (m, 4H, C^βH₂), 2.20 (s+d, ²*J*_{Pt,H} = 70.6 Hz, 6H, PtCH₃), 2.99 (s(br), 4H, C^αH₂), 3.55 (m, 16H, C^εH₂), 3.74 (t, 4H, C⁸H₂), 4.32 (t, 4H, C⁹H₂), 6.7 (s(br), 2H, NH₂), 7.21 (m, 2H, C⁵H), 7.35 (m, 2H, C⁶H), 7.49 (d, ³*J*_{H,H} = 8.3 Hz, 2H, C⁷H₂), 7.94 (d, ³*J*_{H,H} = 8.3 Hz, 2H, C⁴H₂), 8.33 (s+d, ³*J*_{Pt,H} = 6.9 Hz, 2H, C²H). ¹³C NMR (125 MHz, CDCl₃): δ -8.3 (PtCH₃), 13.6 (s, C^γH₂CH₃), 20.0 (s, C^γH₂), 28.2 (s, C^βH₂), 45.9 (s, C⁸H₂), 49.0 (s, C^αH₂), 69.4 (s, C⁹H₂), 70.6 (s, C^εH₂), 70.7 (s, C^εH₂), 70.9 (s, C^εH₂), 71.2 (s, C^εH₂), 110.8 (s, C⁷H), 121.4 (s, C⁴H), 123.1 (s, C⁵H), 124.0 (s, C⁶H), 134.1 (s, C^{7a}), 140.5 (s, C^{3a}), 147.3 (s, C²H). ¹⁹⁵Pt NMR (107 MHz, CD₂Cl₂): δ -2324 (s). Positive mode ESI-FTICR-MS (CH₂Cl₂/MeOH, 1:10): *m/z* 994.25737 [11+Bu₂NH₂]⁺, calcd for [C₂₈H₄₀⁷⁹Br₂N₄O₅¹⁹⁴Pt+Bu₂NH₂]⁺ 994.25823.

3.4.9. Reaction of [(PtBr₂Me₂)_n]/L12 (→12) with [Bu₂NH₂][PF₆]. ¹H NMR (400 MHz, CD₂Cl₂): δ 2.16 (s+d, ²*J*_{Pt,H} = 71.4 Hz, 6H, CH₃), 3.40 (m, 24H, C^εH₂), 3.70 (t, 4H, C⁷H₂), 4.11 (s(br), 3.2H, C⁸H₂), 4.18 (s(br), Ph-CH₂), 4.30 (t, 0.8H, C⁸H₂),

Table 5. Crystallographic and Data Collection Parameters for 8•2CH₂Cl₂, 9•CHCl₃ and 10•CH₂Cl₂

	8•2CH ₂ Cl ₂	9•CHCl ₃	10•CH ₂ Cl ₂
empirical formula	C ₃₈ H ₄₄ Br ₄ Cl ₄ N ₈ Pt ₂	C ₂₁ H ₂₅ Br ₂ Cl ₃ N ₄ OPt	C ₂₃ H ₃₀ Br ₂ Cl ₂ N ₄ O ₂ Pt
<i>M</i> _r	1464.43	810.71	820.32
cryst syst	triclinic	monoclinic	triclinic
space group	<i>P</i> $\bar{1}$	<i>P</i> 2 ₁ / <i>n</i>	<i>P</i> $\bar{1}$
<i>a</i> /Å	13.2372(4)	13.0583(2)	9.9990(4)
<i>b</i> /Å	14.0095(2)	10.2477(2)	10.9524(3)
<i>c</i> /Å	14.3908(4)	18.9450(4)	13.043(1)
α /deg	66.918(2)	90	86.17
β /deg	65.290(3)	103.107(2)	67.837(3)
γ /deg	87.680(2)	90	84.563(3)
<i>V</i> /Å ³	2265.8(1)	2469.13(8)	1316.1
<i>Z</i>	2	4	2
<i>D</i> _{calcd} /g•cm ⁻³	2.208(1)	2.181	2.07
<i>T</i> /K	130(2)	130(2)	130(2)
μ (Mo K α)/mm ⁻¹	10.240	9.267	8.599
<i>F</i> (000)	1384	1544	788
θ range/deg	2.70–28.28	2.55–28.28	2.56–28.28
no. of rflns collected	57 303	61 927	29 411
no. of indep rflns	10 927	6136	5781
no. data/restr/params	10 927/10/558	6136/0/291	6526/0/309
goodness-of-fit <i>F</i> ²	0.940	1.051	1.03
<i>R</i> ₁ , <i>wR</i> ₂ (<i>I</i> > 2 σ (<i>I</i>))	0.0276, 0.0504	0.0196, 0.0395	0.0167, 0.0373
<i>R</i> ₁ (all data)	0.0508, 0.0557	0.0284, 0.0430	0.0214, 0.0390
largest diff peak and hole/e•Å ⁻³	1.744, -1.272	1.693, -0.842	0.755, -0.943
<i>T</i> _{min} / <i>T</i> _{max}	0.324/1.000	0.589/1.000	0.307/1.000

4.55 (m, Ph-CH₂), 6.97 (m, 0.8H, C⁵H), 7.13 (m, 1.2H, C⁵H), 7.25 (m, 2H, C⁶H), 7.32 (m, 10H, Ph-H), 7.55 (m, 2H, C⁷H₂), 7.83 (d, ³*J*_{H,H} = 8.3 Hz, 2H, C⁴H₂), 8.32 (s(br), 2H, C²H). ¹³C NMR (100 MHz, CD₂Cl₂): δ -8.2 (s, CH₃), 45.2 (s, C⁸H₂), 52.5 (s, Ph-CH₂), 52.9 (s, Ph-CH₂), 68.5 (s, C⁹H₂), 70.4 (m, C^eH₂), 110.6 (s, C⁷H), 121.2 (s, C⁴H), 123.1 (s, C⁵H), 124.2 (s, C⁶H), 129.0 (s, C, Ph), 129.3 (s, C, Ph), 129.7 (s, C, Ph), 130.1 (s, C, Ph), 130.5 (s, C, Ph), 130.6 (s, C, Ph), 131.3 (s, C, Ph), 132.4 (s, C, Ph), 133.7 (s, C^{7a}), 140.2 (s, C^{3a}), 146.9 (s, C²H). ¹⁹⁵Pt NMR (107 MHz, CD₂Cl₂): δ -2327 (s). Positive mode ESI-FTICR-MS (CH₂Cl₂/MeOH, 1:3): *m/z* 1150.28091 [12+Bn₂NH₂]⁺, calcd for [C₃₂H₄₈⁷⁹Br₂N₄O₇¹⁹⁴Pt+Bn₂NH₂]⁺ 1150.27937.

3.4.10. Reaction of [(PtBr₂Me₂)_n/L12 (→12) with [Bu₂NH₂]-[PF₆]. ¹H NMR (400 MHz, CD₂Cl₂): δ 0.93 (t, ³*J*_{H,H} = 7.5 Hz, 6H, C⁷H₂CH₃), 1.35 (m, 4H, C⁷H₂), 1.58 (m, 4H, C⁸H₂), 2.15 (s+d, ²*J*_{Pt,H} = 71.2 Hz, 1.8H, PtCH₃), 2.16 (s+d, ²*J*_{Pt,H} = 71.4 Hz, 4.2H, PtCH₃), 2.99 (s(br), 4H, C⁹H₂), 3.52 (m, 24H, C^eH₂), 3.76 (t, 4H, C⁸H₂), 4.34 (t, 4H, C⁹H₂), 6.90 (s(br), 2H, NH₂) 6.98 (m, 0.6H, C⁵H), 7.07 (m, 1.4H, C⁵H), 7.24 (m, 2H, C⁶H), 7.47 (d, ³*J*_{H,H} = 8.3 Hz, 2H, C⁷H₂), 7.62 (m, 0.6H, C⁴H₂), 7.73 (d, ³*J*_{H,H} = 8.4 Hz, 1.4H, C⁴H₂), 8.39 (s(br), 2H, C²H). ¹³C NMR (125 MHz, CDCl₃): δ -8.1 (PtCH₃), 13.8 (s, C⁷H₂CH₃), 20.0 (s, C⁷H₂), 28.7 (s, C⁸H₂), 45.8 (s, C⁸H₂), 48.9 (s, C⁹H₂), 68.9 (s, C⁹H₂), 70.7 (m, C^eH₂), 110.8 (s, C⁷H), 121.2 (s, C⁴H), 123.0 (s, C⁵H), 124.0 (s, C⁶H), 133.8 (s, C^{7a}), 140.4 (s, C^{3a}), 147.0 (s, C²H). ¹⁹⁵Pt NMR (107 MHz, CD₂Cl₂): δ -2330 (s), -2329 (s). Positive mode ESI-FTICR-MS (CH₂Cl₂/MeOH, 1:3): *m/z* 1082.31531 [12+Bu₂NH₂]⁺, calcd for [C₃₂H₄₈⁷⁹Br₂N₄O₇¹⁹⁴Pt+Bu₂NH₂]⁺ 1082.31067.

3.5. In Vitro Studies. The cells for the cytotoxicity assay and platinum uptake studies were cultivated in the Biozentrum, Martin-Luther-Universität Halle-Wittenberg. The cells for the trypan blue exclusion test were cultivated in the Hämatologisch/Onkologisches Forschungslabor, KIMIV, Martin-Luther-Universität Halle-Wittenberg.

3.5.1. Cell Cultures. Three different cell lines were used in this work: liposarcoma, A549 (lung carcinoma) and 518A2 (human melanoma). The cells were cultivated in medium: D-MEM with FBS (50 mL in 500 mL D-MEM) and penicillin/streptomycin 5 mL in 500 mL of D-MEM (all purchased from Gibco-Invitrogen).

3.5.2. Cytotoxicity Assay. All stock solutions of the compounds (20 mg/mL) were prepared in DMF, except **3**, which was prepared in DMSO (final concentration of DMF/DMSO in the medium <0.01% v/v). The drug concentration that reduced the number of living cells by 50% is defined as IC₅₀. The IC₅₀ values were obtained

as follows: 25 000 cells were plated in Petri dishes (diameter 6 cm). After 24 h the clean medium was replaced by medium spiked with the compound. After 72 h incubation at 37 °C in a fully humidified atmosphere containing 5% CO₂ the spiked medium was removed and the surviving cells were counted after trypsinisation. The procedure was repeated in triplicate.

3.5.3. Measurement of Platinum Uptake. 250 000 cells were seeded in Petri dishes (diameter 15 cm) and incubated for 24 h with clean medium (as above). Stock solutions of the compounds were prepared as described in "Cytotoxicity Assay". After 24 h the medium was replaced by medium spiked with the compound (ca. IC₅₀) and the cells were incubated a further 24 h. The cells were washed, trypsinated, centrifuged and lyophilized, and the platinum content was measured using a solid sampling graphite furnace with SS-GF AAS model AAS5 EA (Jena GmbH, Germany) by ramping the temperature from 100 to 2250 °C and measuring at λ = 265.9 nm.

3.5.4. Determination of Apoptosis. Determination of programmed cell death was performed using the trypan-blue exclusion method. Human tumor cell lines liposarcoma, A549 and 518A2 were exposed to equitoxic IC₉₀ drug doses (according to cytotoxicity studies of a 72 h treatment regime) and detached (floating) cells were harvested and analyzed after different time periods. If IC₉₀ doses were not reached, respective IC₇₀ or IC₅₀ values were used. Apoptotic cell death was proven by the ability of cells to exclude trypan-blue (trypan-blue solution (0.4%), Sigma-Aldrich, Germany).

3.6. X-ray Crystallography. Single crystals of **2**•2THF were grown by slow diffusion of an MeCN solution of **L2** into a THF solution of [PtBr₂Me₂(THF)₂] at 4 °C for two weeks and room temperature for one week. Similarly, single crystals of **8**•2CH₂Cl₂ were grown by slow diffusion of a CH₂Cl₂ solution of **L8** into a MeOH solution of [PtBr₂Me₂(MeOH)₂] at room temperature over two weeks. Single crystals of **5** were obtained from a mixture of KBF₄ and **5** stored at room temperature in MeOH for several weeks. Crystals of **3**•CHCl₃, **9**•CHCl₃ and **10**•CH₂Cl₂ crystallized from solutions (CHCl₃: **3** and **9**; CH₂Cl₂: **10**) of the respective complex left to partially evaporate at room temperature. Tables 4 and 5 show crystallographic and data collection parameters. Intensity data were collected on either a Stoe-IPDS (**2**•2THF and **3**•CHCl₃) or a CCD Xcalibur S diffractometer (**5**, **8**•2CH₂Cl₂, **9**•CHCl₃ and **10**•CH₂Cl₂) both with Mo K α radiation (λ = 0.7103 Å, graphite monochromator). Absorption corrections for **2**•2THF and **3**•CHCl₃ were made using the IPDS software package.^{27a} Semiempirical absorption

corrections were carried out for **5**, **8**·2CH₂Cl₂, **9**·CHCl₃ and **10**·CH₂Cl₂ with SCALE3 ABSPACK.^{27b} All structures were solved by direct methods with SHELXS-97²⁸ and refined using full-matrix least-squares routines against F^2 with SHELXL-97.²⁸ The solvent molecules of **8**·2CH₂Cl₂ were disordered; Cl2 was refined over three different positions, as were Cl3 and Cl4 of the second solvent molecule, using DFIX and FREE instructions for suitable refinement. Non-hydrogen atoms were refined with anisotropic displacement parameters. Hydrogen atoms were included in the models by calculating the positions using the riding model and were refined with isotropic displacement parameters. Illustrations were generated using Diamond 3.0 software.²⁹

Crystallographic data for the structures reported in this paper have been deposited with the Cambridge Crystallographic Data Centre, CCDC-682023 (**2**·2THF), CCDC-682024 (**3**·CHCl₃),

CCDC-682025 (**5**), CCDC-682026 (**10**·CH₂Cl₂), CCDC-682027 (**9**·CHCl₃) and CCDC-682028 (**8**·2CH₂Cl₂). Copies of this information may be obtained free of charge from The Director, CCDC, 12 Union Road, Cambridge CB2 1EZ, UK (fax: +44-1223-336033; e-mail: deposit@ccdc.cam.ac.uk or <http://www.ccdc.cam.ac.uk>).

Acknowledgment. The authors acknowledge the Deutsche Forschungsgemeinschaft for financial support, Dr. Ströhl for NMR measurements and useful discussion and Merck for gifts of chemicals.

Supporting Information Available: CIFs giving X-ray crystallographic data, tables showing selected bond lengths of all structures herein and selected bond angles of **2**·2THF, **3**·CHCl₃ and **5**. Details of NOE experiments, extra data relating to ESI-FTICR-MS and infrared spectral data are also included and are available free of charge via the Internet at <http://pubs.acs.org>.

OM800323Z

(28) Sheldrick, G. M. *Acta Crystallogr.* **2008**, *A64*, 112.

(29) Branderburg, K. *Diamond*, Release 2; Crystal Impact GbR, Bonn, 1997.